ADVANCED OPTICAL MATERIALS
www.advopticalmat.de

Microresonators in Lithium Niobate Thin Films

Ran-Ran Xie, Gui-Qin Li, Feng Chen, and Gui-Lu Long**

Leveraging the outstanding nonlinear optical properties and the ultra-high spatial confinement of light, microresonators based on lithium niobate (LN) thin films have emerged as intriguing elements in various frontiers such as integrated photonic circuits and quantum photonics. A number of applications have been realized based on LN thin-film microresonators toward various on-chip devices. In this paper, the recent advances of microresonators based on LN thin films are reviewed, including essential techniques used in fabrication/characterization and a detailed overview of applications, ranging from frequency conversion, electro-optic modulation, frequency combs, microwave-to-optical transducers, quantum photonics, to lasing. A short summary and perspective is presented to indicate possible research topics related to LN thin-film.

1. Introduction

Microresonators[1–3] are key devices for modern photonics toward a large variety of applications, for example, lasers,[4–8] nonlinear optics,[9–14] cavity optomechanics,[15–19] sensing,[20–23] and quantum information processing.[24–28] Benefiting from the geometries of microcavities supporting "whispering gallery modes" (WGMs) the light field can be confined in extremely small volumes, reaching very high power density and very narrow spectral linewidth. As a result, the ultrahigh in-cavity intensities significantly enhance the photon-to-photon interactions, leading to ultrahigh efficiencies of nonlinear optical process even at low-power optical excitation. In addition, the small scale enables the construction of resonator-based functional devices with very high integration. With combination of these intriguing features, low-power-consumption, low-cost on-chip devices can be developed successfully. The material platforms for microresonators are crucial for the practical applications. For example, silicon dioxide (SiO_2) is considered as one of the most commonly used materials for microresonators, and great success has been achieved based on this easy-to-fabricate platform.[29,30] Recently, with the well-developed technology for on-chip circuits fabrication, some semiconductor materials have been harnessed as the platforms of microresonators for more electro-optic potentials, such as silicon (Si),[31,32] SiC,[33–36] ZnO,[37,38] GaN,[39,40] or AlN[41,42]. Among them, lithium niobate ($LiNbO_3$ or LN) has risen into the forefront of microresonator demonstrations and drawn extensive interests in photonics and electronics.

Lithium niobate is a multi-functional dielectric crystal that combines a number of excellent features,[43] such as electro-optic, nonlinear optical, acousto-optic, ferroelectric, piezoelectric, photorefractive, photo-luminescent properties, and receives a broad variety of applications in telecommunication, frequency conversion, optical storage, filtering, and quantum photonics.[44–47] The single-crystal thin film of LN is an ideal platform for microresonators owing to the unique combination of various excellent properties of the bulk. The major obstacle of the LN-based microcavities was the fabrication of high-quality LN thin films because the single-crystalline features cannot be well-preserved in thin-film LN produced by chemical methods of normal deposition that is applied for semiconductors. In addition, large-scale LN-thin film wafers are desired for further processing of on-chip devices. Recently, the so-called "lithium niobate on insulator" (LNOI) technology figures the major problem out and boosts the rapid development of the thin-film LN based devices.[48–53] Most used LN films are manufactured by smart " Ion cut" technique. The typical commercialized LN thin film based on ion cut consists of a single-crystalline LN thin film with thickness of 300-900 nm, a cladding layer of SiO_2 with thickness of 2–3 μm, and the supporting material (LN or Si bulk wafer). The fabrication process of ion-cut LN thin film can be referenced in details elsewhere.[54–56] The refractive

R.-R. Xie, Prof. G.-Q. Li, Prof. G.-L. Long
Department of Physics
Tsinghua University
Beijing 100084, P. R. China
E-mail: gllong@tsinghua.edu.cn
R.-R. Xie, Prof. G.-L. Long
State Key Laboratory of Low-Dimensional Quantum Physics
Tsinghua University
Beijing 100084, P. R. China
Prof. F. Chen
School of Physics, State Key Laboratory of Crystal Materials
Shandong University
Jinan 250100, P. R. China
E-mail: drfchen@sdu.edu.cn
Prof. G.-L. Long
Frontier Science Center for Quantum Information
Beijing, P. R. China
Prof. G.-L. Long
Beijing National Research Center for Information Science and Technology
Beijing, P. R. China
Prof. G.-L. Long
Beijing Academy of Quantum Information Sciences
Beijing, P. R. China
Prof. G.-L. Long
School of Information
Tsinghua University
Beijing, P. R. China
The ORCID identification number(s) for the author(s) of this article can be found under https://doi.org/10.1002/adom.202100539.

DOI: 10.1002/adom.202100539

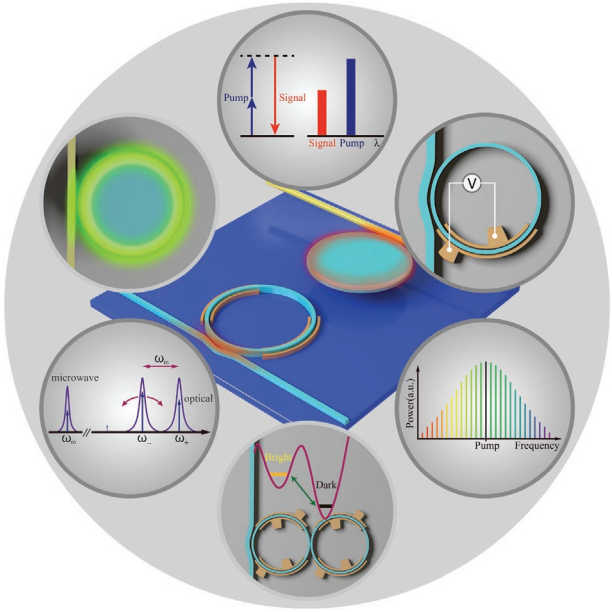

Figure 1. Schematic illustration of microresonators based on LN thin films.

index contrast (Δn) of LN and cladding SiO_2 layer is as high as 0.6, which enables fabrication of low bending loss of microcavities (e.g., microrings or microdisks). The thickness of LN thin film is less than 1μm, which allows very tight confinement of light field in very small volumes; consequently, light-light interaction is significantly enhanced. So far, owing to the rapid development of LNOI technology, high-quality, wafer-scale (up to 6 inch wafer) LN films[57] have been available, offering substantial platforms to produce thin-film LN based devices for diverse applications.

In this paper, we review the state-of-the-art advances of microresonators based on LN thin films, including the fabrication, characterization, and applications (**Figure 1**). First, a brief overview of the thin-film LN-based microresonators and the used fabrication solutions are presented. Second, we introduce the fundamental schemes to solve vital obstacles in experiments like how to satisfy phase matching condition. Third, several selected applications are presented, including frequency conversion, electro-optic modulation, frequency combs, micro-to-optical transducers, quantum photonics and lasing. Finally, a short summary and perspective is given to indicate some possible topics of future research related to thin-film LN-based microresonators.

2. Fabrication and Investigation Techniques

2.1. Quality Factors and Fabrication Methods

For microresonators, quality factor (Q) is a key parameter to benchmark the ability in storing light. The strict light confinement boosts light-matter-interaction, and decreases the thresholds of nonlinear effects. One of the fundamental tasks in harnessing LN thin film microresonators is to achieve a Q factor as high as possible. The quality factor is denoted by $Q = \omega_{cav}/\kappa$, where ω_{cav} and κ are the resonance frequency and decay rate, respectively. The total decay rate κ is composed of two main losses: the coupling loss rate κ_{ex} and the intrinsic loss rate κ_0. The former refers to the damping between the microresonator and the waveguide. While the latter indicates the loss inside a microresonator including material absorption, radiation loss and scattering energy loss. Experimentally, the roughness of the resonator surface like lattice disorders and periphery imperfections may strongly scatter light out of resonators, which limits the quality factor significantly. Thus the issue to realize high-Q LN microresonators lies on how to smooth the surface of resonators.

Since the first optical microring resonator in submicrometre thin film of LN was realized in 2007,[66] a variety of fabrication methods have been employed to achieve ultralow roughness and the quality factor of LN microresonators has already reached above 10^8 (intrinsic).[65] **Table 1** summarizes the relevant parameters for some typical recent experimental implementations of high-Q microresonators. In the early days, an undercut microdisk structure was demonstrated by using selective ion implantation assisted wet etching from a crystalline LN substrate.[67] Under the diluted HF solution, etching would proceed laterally along the ion resident layer leading to a undercut structure formed. During a high temperature annealing, surface tension smoothed and reshaped the microdisk edge with a Q factor of 2.6×10^4. Nevertheless, the aforementioned method is not suitable for batch-fabrication. As LNOI wafer developed by ion slicing and wafer bonding techniques has risen into commercial production, based on which fabrication tech-

Table 1. Experimental parameters for a representative sampling of published literatures.

Type	Processing method	Cut direction	Thickness [μm]	Diameter [μm]	Ridge width [μm]	Quality factor (loaded)	Wavelength [nm]	Ref.
Disk	RIE	–	0.5	79.2	–	1.19×10^6	1550 band	[58]
Ring	RIE	z-cut	0.7	200	7	3.0×10^6	976	[59]
Racetrack	ICP RIE	x-cut	0.6	–	2.4	5.0×10^6	1590	[60]
Ring	Argon ion milling	x-cut	0.49	120	1.2	1.3×10^6	1493.11	[61]
Disk	FIB	x-cut	0.6	29.92	–	9.61×10^6	1547.8	[62]
Disk	FIB	z-cut	0.3	50	–	8.2×10^5	1535	[63]
Disk	Wet etching	–	0.4	20	–	2.2×10^5	1550 band	[64]
Disk	CMP	x-cut	0.6	1060	–	7.5×10^7	1551.52	[65]

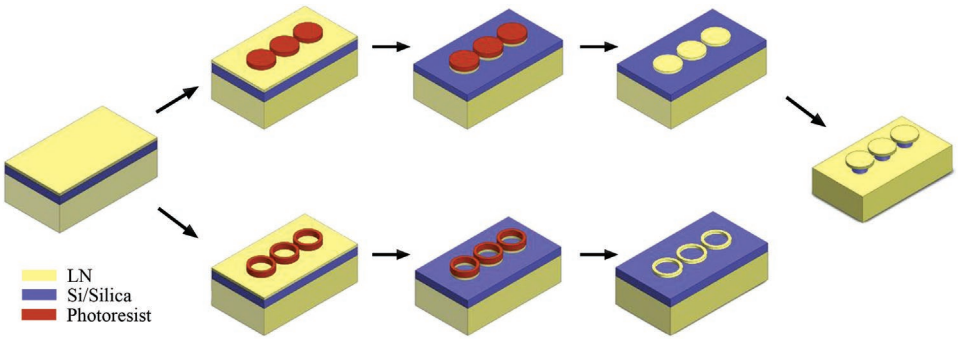

Figure 2. Fabrication procedure of microdisks (upper) and microrings (lower): writing the pattern in a mask layer; ion dry etching to transfer the pattern to the LN thin film; removing mask layer; undercut etching only for microdisks.

niques like ion dry etching, focused ion beam milling (FIB) and chemical-mechanical polishing (CMP) have been used to make high-Q microresonantors. Surface roughness of samples can be well suppressed by processing of these three techniques, successfully enhancing the Q factor to be above 10^5. In this work, we mainly introduce these three fabrication processes.

Ion dry etching is a convenient method in standard nanofabrication due to its controllable and high etching rates of several tens of nanometers per minute. The fabrication procedure is schematically illustrated in **Figure 2**. First, the process starts from the LNOI wafer with a sandwiched structure. Between LN thin film and bulk LN substrate there is an insulating layer which usually uses silica. Second, the pattern is written in a mask layer. In this step, either UV lithography[58] or electron-beam lithography[68–70] can be utilized to obtain clear and sharp edges for the mask. Then, the dry etching is introduced to transfer this pattern onto the LN thin film. Many groups are using argon plasma milling and reactive ion etching (RIE)/inductively coupled plasma reactive ion etching (ICP RIE) to etch LN thin film. Next, after removing the mask layer, microstructures have been formed in LN thin film. For microrings, the fabrication process is completed. While as for microdisks, undercut etching is required to enable the microdisks free-standing (only supported by pillars). The choice of undercut etching depends on the used insulating material, typically HF solution for silica[71] and XeF_2 for silicon.[72] In this recipe, many etching parameters such as gas ratio, pressure, power are optimized to reach the perfect smoothness for minimizing the scattering loss. Besides, the size and shape of microresonators also impact the Q factors. By setting the racetrack microresonator with perfect widths and straight section lengths, an ultra-high-Q optical cavity with the intrinsic Q above 10^7 has been realized (**Figure 3**).[60] All these techniques or devices in ion dry etching method are batch production compatible propelling the commercial development of LN thin film based microresonators. It should be noted that the inevitable surface defects during ion etching process truly can set some roadblocks when it comes to superior high-Q cavities.

FIB milling is a highly precise technique in sub-micron fabrication, which has been applied for many complicated on-chip photonic devices. The first microresonator in LN thin film prepared by FIB was proposed in 2015 corresponding to the quality factor of 2.5×10^5.[73] The FIB millling was operated twice consecutively to smooth the rough periphery (a few tens of nanometers) of cylindrical posts formed by the femtosecond laser ablation. **Figure 4** shows the SEM (scanning electron microscope) image of the sidewalls of the microresonator before and after the FIB milling. Later the same group successfully improved the quality factor to 2.45×10^6 by optimizing the milling current (1 nA) and the duration of the post-annealing (500 °C for 4 h).[74] Although FIB is well suitable for fabricating structures in demand of high resolution, the operation area is typically up to hundreds of square microns, not big enough for large-scale on-chip photonic devices which restricts its practical application forward.

As an alternative to FIB milling, CMP[75] gets the rid of size limitation and has become another competitive solution to machine ultra-high microdisks in LN thin films. The fabrication process mainly includes four steps: coating a Cr thin film on top of the LNOI as a hard mask, patterning the Cr thin film into a microdisk by femtosecond laser ablation, transferring the disk-shaped pattern to LNOI by CMP, removing the Cr film thin film and the sillica buffer layer with chemical wet etching (**Figure 5**a).[76] In this experiment, the Q-factor was measured as 1.46×10^7 for a microdisk with the diameter of 140 μm. Without spoiling the Q factor, the angle between sidewall and the vertical direction can be modified continuously from 9° to 51° by adjusting the polishing duration (Figure 5b),[77] which is crucial in nonlinear frequency comb generation (see Section. 3.3 for more details). By applying CMP to both thin-film preparation and micro-resonator fabrication for mitigating ion-implantation induced lattice damage, the average surface roughness was reduced to less than 0.5 nm. Arising from this superior smoothness, the intrinsic quality factor reached 1.5×10^8, which is the highest Q factor in reported literatures.[65]

To improve the Q factor as far as possible even after fabrication, some post-process annealing methods are proposed. Besides high temperature reheating, femtosecond laser modification was also used as another novel "light annealing" method.[78] After fabrication, the femtosecond laser was focused on the middle between the periphery and the center of the microdisk. By means of the laser spot, a tiny defect on the top side appeared, thanks to which the following laser pulses were scattered into the cavity modes to further smooth the sidewall of the microdisk. Other than the demonstrations benefited from smart ion slicing and wafer bonding technique above, there are still some heterogenerous microresonator structures on LN thin film that both capitalize the excellent quality and

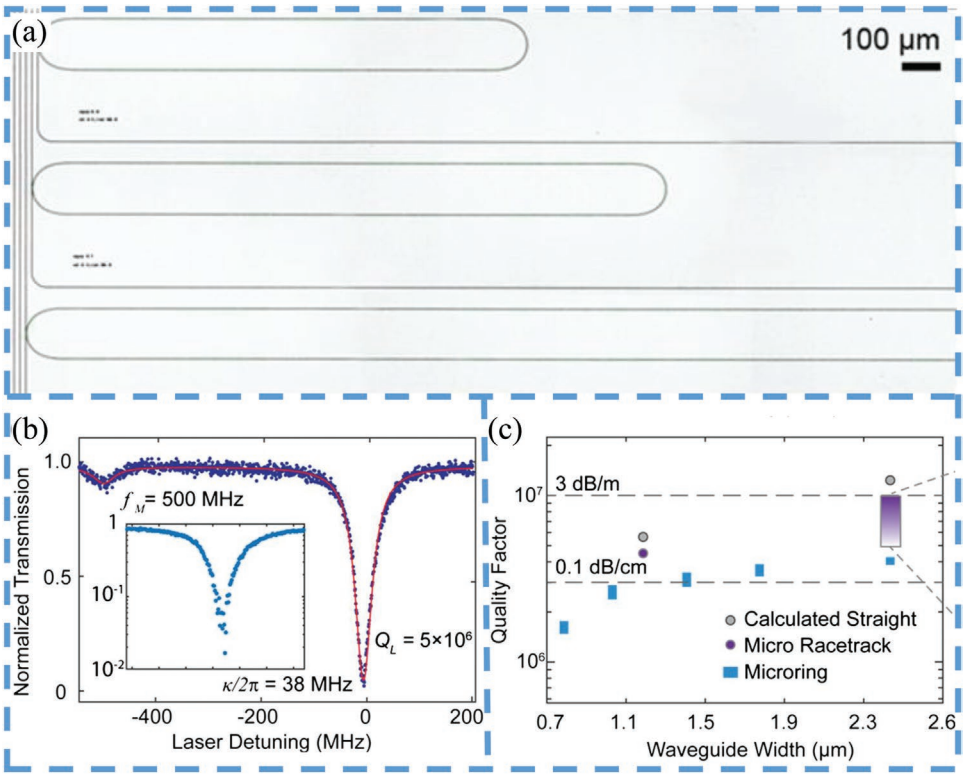

Figure 3. a) Optical microscope image of micro-racetrack resonators of various lengths. b) Transmission of the best device with loaded $Q_L = 5 \times 10^6$. c) Measured quality factors for different resonators on several chips. Reproduced with permission.[60] Copyright 2017, The Optical Society.

bypass the fabrication difficulty of LN materials. For these hybrid platform, the complex photonic devices are designed and fabricated in other easy-to-etch material, whether built on the top of a LN thin film layer[79,80] or coated by a thin LN layer later.[81] On the other hand, the hybrid structure is also the Achilles heel: this part of light confined in easy-to-etch materials determines a modest utilization rate of LN features and an inevitable energy loss. This technological expedient would give way to the aforementioned mainstream of fabrication methods as ion dry etching, FIB milling and CMP.

To better capitalize the high-Q microresonators in LN thin film, it is highly demanded to couple light in and out with low loss, wide bandwidth and good robustness. The methods vary with different types of resonators. In regard to microdisks, the free-standing structure can be directly coupled by a tapered fiber.[82] In view of the unequal refractive indexes of silica and LN, the tapered fiber is usually put in contact with the microdisk either near the rim or on the top surface to maximize the mode overlap for high coupling efficiency.[69,71,76,81] With regards to ring microresonators, another LN waveguide structure is also fabricated near the circumstance on the same chip meanwhile, with a fixed coupling rate hinging on the gap between the waveguide and the microring. For this case, a choke point lies on the coupling between the LN waveguide and commercial optical fiber as a result of the light filed mismatching. To deal with this problem, the edge coupling[83–87] and grating couplers[88–93]

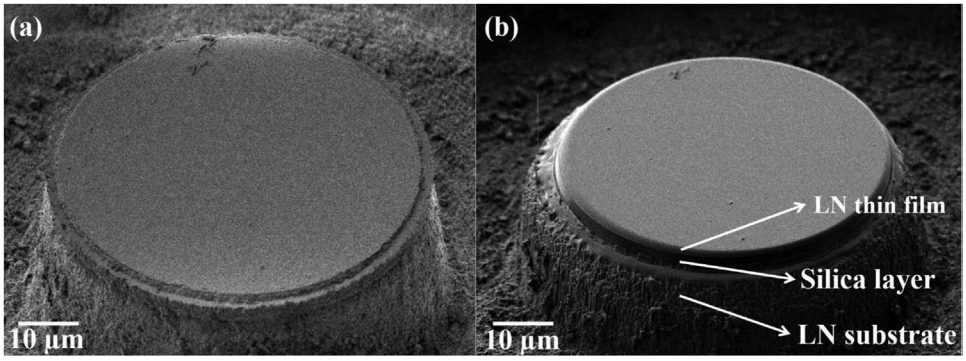

Figure 4. a) SEM image of a cylindrical post formed after femtosecond laser ablation. b) SEM image of the cylindrical post after the FIB milling. Reproduced with permission.[73] Copyright 2015, Springer Nature.

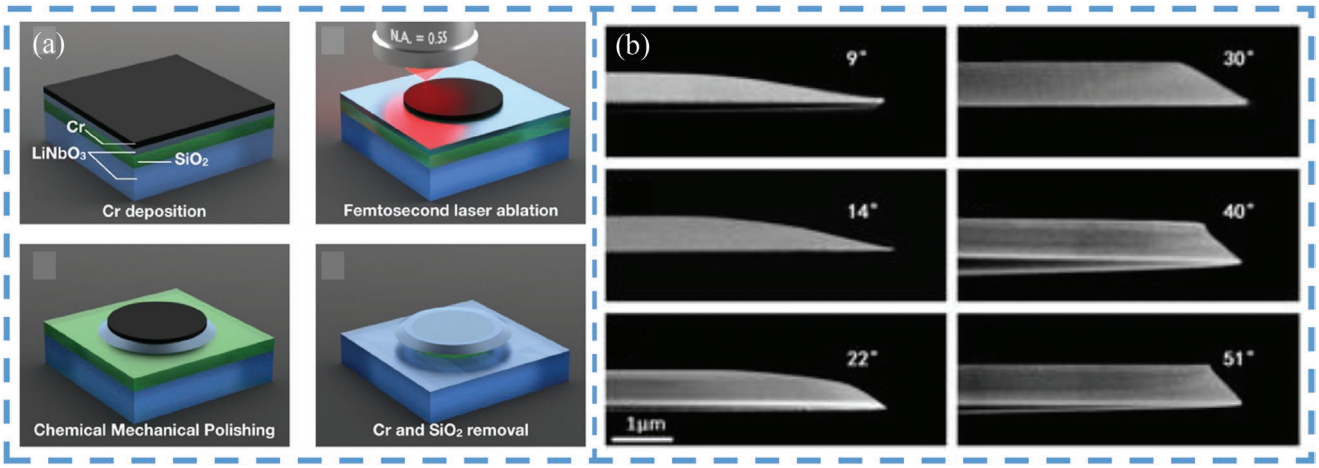

Figure 5. a) Illustration of CMP fabrication flow. Reproduced with permission.[76] Copyright 2018, The Optical Society. b) Side view SEM image of microdisks with different wedge angles. Reproduced under the terms of the Creative Common CC BY license.[77] Copyright 2019, Multidisciplinary Digital Publishing Institute.

have been well studied. Edge coupling is a straightforward way where a lensed fiber is spotted on the cross section of LN waveguide. The coupling efficiency strongly depends on the mode match, thus many ingenious designs have been proposed to optimize the mode shape. Recently, a cladding waveguide (silicon oxynitride) and an ultra-high numerical aperture fiber have been introduced into the edge coupling method where an extremely low coupling loss of 0.54/0.59 dB per facet for TE/TM (transverse electric/magnetic) light has been observed.[87] To our knowledge, this record is the lowest among all published edge coupling schemes. Compared with edge coupling, grating couplers have no quest on precise alignment and smooth facet polishing: the fiber can be set anywhere over the grating region. The increasing convenience from this plug-in connection method truly broadens the applications of LN thin film microresonators in large-scale integrated photonic circuits. Unfortunately, the efficiency of vertical grating coupler is still insufficient. Under this circumstance, many schemes have been employed to enhance the coupling efficiency, including adding another bottom reflective layer to decrease the scattering loss,[88,92] building chirped grating structures to reduce the mode mismatch loss and internal reflection,[90,92] drawing 2D grating patterns.[94]

2.2. Phase Matching Methods

A major issue in implementing the nonlinear optical qualities of LN is to preserve momentum conservation, which is also called as phase matching condition. For simplicity, we consider second-harmonic generation (SHG) as an example. Once the perfect phase matching condition $\Delta k = 2k_p - k_s = 0$ ($k_{p,s}$ indicates the wavevector of pump laser or signal laser) was satisfied, the most wave energy would be extracted from the incident waves with the highest conversion efficiency. With the energy conservation $\omega_s = 2\omega_p$, the perfect phase matching condition requires the refractive indexes of pump and signal laser to fulfil $n(\omega_s) = n(\omega_p)$. To compensate the phase mismatching, techniques such as modal phase matching (MPM),[95,96] cyclic phase matching (CPM)[97,98] and quasi phase matching (QPM)[99–102] have been developed in LN thin film microresonators.

Traditionally, the most common method for phase matching is utilizing the birefringence shown in crystals. For the case of negative uniaxial crystal as LN, the type I phase matching ($o + o \rightarrow e$) and the type II phase matching ($o + e \rightarrow e$) both can be used. For MPM, the pump and signal light should be elaborately selected either for using the birefringence effect or for modes with different orders. The abundance of modal structure inside cavities helps to ease the difficulty of searching. In a z-cut microdisk, the TM mode has its polarization direction perpendicular to the disk plane, experiencing the extraordinary refractive index n_e. While the TE mode obtains the fixed ordinary refractive index n_o. Based on this device, type I phase matching has been achieved by regarding TE mode and TM mode as the pump and signal light respectively in SHG process.[103] However, this kind of crossing polarized light pair method falls short on limited efficiency as it has to utilize the off-diagonal coefficient rather than the strongest $d_{33} = 27pM/V$. To deal with this, parallel polarized modes with different orders are introduced to satisfy the phase match by designing the cross section shape of microrings. Recently, Chen et al. and Luo et al. utilized TM_0 mode as pump light and TM_2 as second-harmonic light in a z-cut LN thin film microring, respectively,[95,96] which belongs to the type 0 phase matching ($e + e \rightarrow e$). In 2016, Lin et al. first applied CPM method[104] in microresonators in LN thin film.[97] In the x-cut LN thin film, the polarization of *TM* modes is perpendicular to the crystalline optical axis, leading to a constant ordinary refractive index. Nevertheless, the refractive index of TE modes oscillates from the ordinary to extraordinary values according to $\frac{1}{n^2(\lambda,\theta)} = \frac{\cos^2\theta}{n_o^2(\lambda)} + \frac{\sin^2\theta}{n_e^2(\lambda)}$. It is clear that the refractive index of TE mode varies with the angle (θ) between the crystalline optical axis and the propagation vector in the period of 2π. In every round trip, there are four azimuthal angles where perfect phase matching takes place, as shown in **Figure 6**. This CPM solution opens new possibility for phase matching in LN thin film microresonators.

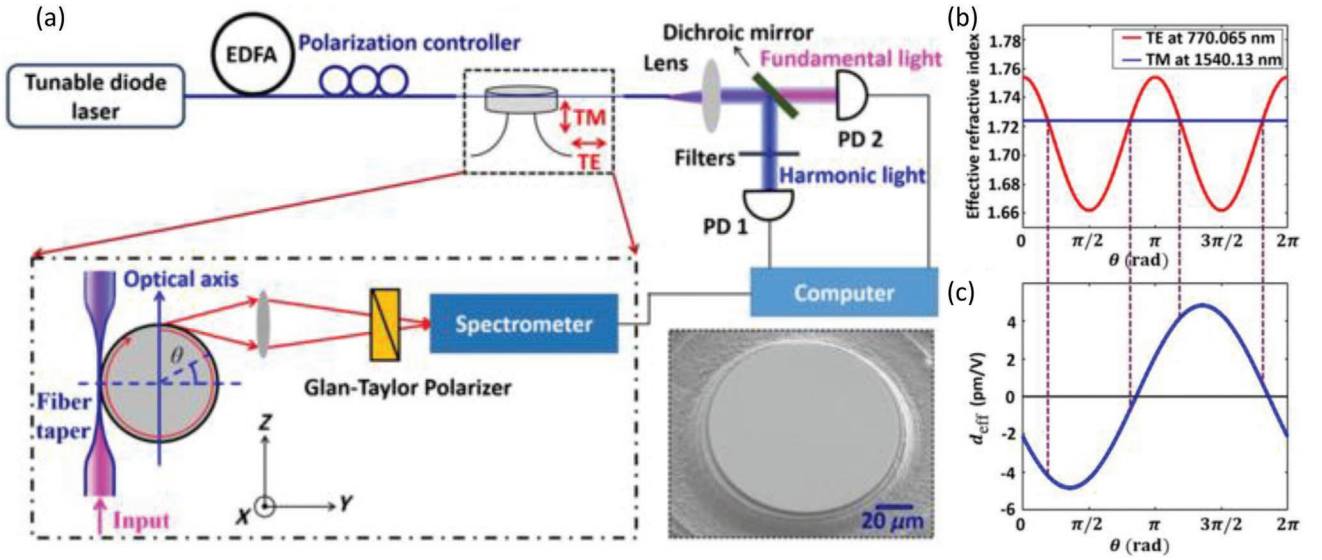

Figure 6. a) Experimental setup using cyclic phase matching. In the inset on the left-hand side, θ indicates the angle between the wave vector and the crystalline optical axis. b) Numerically calculated effective refractive indices of the pump (solid blue curve) and second-harmonic modes (red dashed curve), c) nonlinear coefficient versus the azimuth angle along the microresonator periphery. Reproduced with permission.[97] Copyright 2016, The American Physical Society.

Since QPM was proposed in 1962,[105] this scheme has been widely used in many circumstances where birefringence effects are not suitable. For example, there still are some particular applications that ask for the utilization of d_{33} to yield an extreme high optical nonlinearity. For these cases, QPM tends to be the best choice to compensate for the phase mismatching. To implement QPM, a periodically poled structure is written to invert the orientation of crystalline axes as a function of position with a distant period Λ, which consequently reverses the sign of coefficient d_{eff}. When the changes of d_{eff} are coincident to the oscillation from the phase mismatching, the output field amplitude continues to grow monotonically. This is actually how QPM works. During QPM, the optimum period of poled structure is $\Lambda = \frac{2\pi}{\Delta k}$. A number of demonstrations of QPM have been reported in LN thin film microresonators. The poling period domain in LN material is fabricated by adding a voltage larger than the coercive electric filed of LN crystal to inverse the spontaneous polarization. The alignment of electrodes lies on the cut direction of LN wafers.[106,107] For a z-cut wafer, the orientation of extra electric field is perpendicular to the wafer surface where a tiny AFM (Atomic Force Microscope)-tip takes effect to write the domain. The equipment scheme is given in **Figure 7**a. As for x-cut wafers, the opposite electrodes are designed in plane of the wafer surface. The inverted pattern is often introduced before the smart ion slicing for thin film, which can also appear as a post-process after the microresonator has already been built.[102] With this dramatic jump in poled domain fabrication techniques, PPLN (periodically

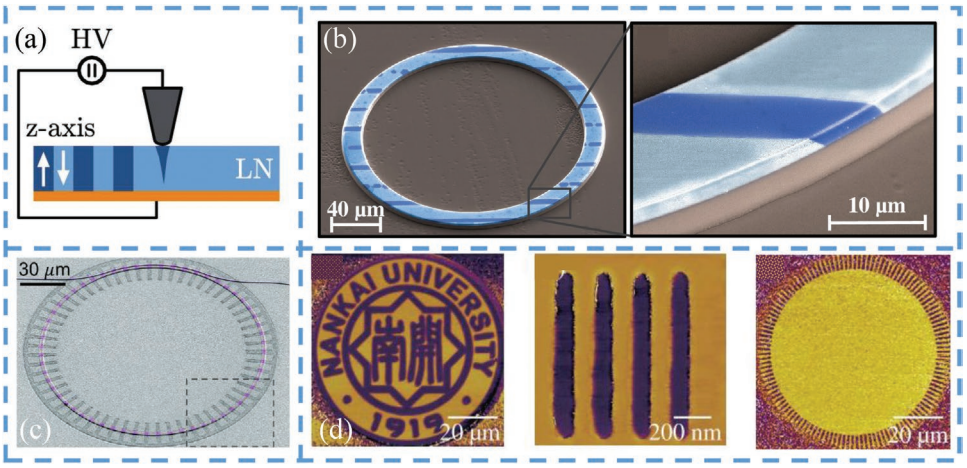

Figure 7. a) Domain inversion in fabrication. b) False-color SEM images of a PPLN on-chip WGR with a diameter of 216 m and zoomed view. Reproduced with permission.[99] Copyright 2018, The Optical Society. c) False-color SEM images of a PPLN microring resonator. Reproduced with permission.[101] Copyright 2019, The Optical Society. d) PFM (piezo force microscopy) image of logo, strips and microdisk. Reproduced with permission.[102] Copyright 2020, The Optical Society.

poled lithium niobate) microresonators came to the world and promoted the further utilization of d_{33} in nonlinear photonic applications.[99,100] Figure 7b,c shows false-color SEM images of PPLN microring resonators. Nowadays, the improvement of domain engineering has already made it possible to satisfy the rigorous requirement for complex domain pattern and in sub-micrometer unit scale, which is illustrated in Figure 7d.

3. Applications

The aforementioned fabrication and investigation techniques clear the way of LN thin film microresonators to be widely utilized for both fundamental physics study and microdevice construction. In this section, we choose several main applications to represent the enormous potentials.

3.1. Frequency Conversion

Frequency conversion is a primary topic in nonlinear optics as well as a necessary quest in integrated photonic devices. The LN thin film based microresonator, as a combination of large second-order susceptibility in LN and high light-matter-interaction in microresonators, makes it feasible to realize an intriguing frequency conversion at a very low pump power. To date, various quadratic nonlinearity have been demonstrated, such as SHG, sum-frequency generation (SFG),[108,109] difference-frequency generation (DFG),[96] and parametric down conversion.[110,111] Among them, SHG is the basic in transferring the wavelength of signal light, which has been deeply researched in microresonators in LN thin film.[68,74,97–103,112–114] To characterize the ability of energy transform, a notable parameter named conversion efficiency is usually given by $\eta = P_s/P_p^2$, where $P_{s(p)}$ denotes the on-chip signal (pump) power. A high conversion efficiency requires tight light confinement, good mode overlapping for all light wavelengths, fully leveraging the nonlinear susceptibility tensor element and choosing optimal phase matching (more information seen in Section. 2.2). Tang's group demonstrated the high SHG efficiency about 250 000%/W in a dual-resonant, periodically poled LN thin film microring resonator, even with the d_{31} coefficient leveraged.[101] Here a pump telecom TE_{00} and a signal near-visible TM_{00} were involved in this SHG process (**Figure 8**a). They employed the thermal tuning to let the dual-resonance condition satisfied because of the distinct difference of frequency shifting when temperature changing. As the function of input light power, the variation of SHG light power and conversion efficiency were investigated (Figure 8b). After carefully fitting, the slope of 1.02 and the efficiency of 250 000%/W were obtained. In addition, there was a saturation about 15% if the on-chip pump power above 115 μW. Recently, the same group reached 5 000 000%/W SH conversion efficiency by utilizing the largest nonlinear susceptibility tensor element d_{33}, which was by far the highest among all the demonstration based on LN thin film microresonators.[114]

Other than pure quadratic nonlinearity, cascaded nonlinearity[59,63,115,116] would appear at a higher input power, offering frequency conversion with more freedom to choose in wavelength ranges. Figure 8c indicates the phenomenon in a frequency converter by accessing cascaded stimulated Raman scattering. With the increase of pump power, laser at other wavelengths except the origin SHG (976 → 488 nm) was observed. The short red shifts (976 → 1040 → 1114 nm) correspond to the stimulated Raman scattering. However, although frequency conversion efficiency has already overseen several orders of magnitude increase, there still are a long road to the theoretical prediction[117] which can be stepped over via further optimization in a range from fabrication details to the fully utilization of nonlinear coefficient.

3.2. Electro-Optic Modulation

In integrated photonic circuits, the resonance wavelength of microresonator modules is required to be tunable in order to match the other embedded devices and adapt reconfigurable tasks. Electro-optic (EO) modulation is a super fast, high efficient method when compared to temperature or stretching tuning. For the case of only considering the lowest-order EO modulation, the optical indicatrix $(1/n^2)_i$ is of the form $\Delta(1/n^2)_i = \sum_j r_{ij}E_j$, where the electro-optic coefficients r_{ij} gives the rate of the optical constant changes with increasing electric filed strength E_j. This kind of linear EO change,also known as Pockels effect, is the underlying principle of EO modulators. Unfortunately, traditional microresonators are often based on centro-symmetric crystals. In materials like silica, such linear EO effect vanishes. In contrast, LN with large linear electro-optic coefficients (the highest value r_{33} = 31 pm V^{-1}), propels itself an innovative platform for EO modulations and other applications.

A pursuit of high speed EO modulation requires the fully utilization of r_{33} and the maximization of overlap between optical mode filed and electrical field. To cope with this, both the selection of mode polarization and the alignment of electrodes should coincide with the LN wafer cut direction. **Table 2** reviews the related information about EO modulators demonstrated on LN thin film microresonators. Clearly, for the cases of z-cut LN, the voltage should be loaded vertically with the TM mode observed to access r_{33}.[66,118,126] In experiment, the microresonator can be put inside a parallel-plate capacitor,[58] or be coated with electrodes on the top and bottom surfaces which is shown as **Figure 9**a.[119] While as for x-cut LN, the electrodes are fabricated in-plane,[120,125] often at the lateral sides of the ring resonators.[121,122,127–129] Parallel to the horizontal electrical field, TE modes are often tested for higher EO tuning rates. Figure 9b gives an example of in-plane electrodes structure. It is noteworthy that here the EO modulator was embedded in an add-drop structure, constituting a tunable narrow-band filter. With a Kerr nonlinear comb (seen Section 3.3 for more information) on the same chip, the function of reconfigured switching has already been realized, which is a meaningful attempt in monolithic photonic circuits.[127] To our knowledge, the highest tuning rate was recognized as 29.2 pm/V where an electrode above the microdisk resonator was linked with the conducting pad on the platform to offering a controlling voltage (Figure 9c).[64] More interesting, depending on the distribution of applied electric field, the TE mode rather than the TM mode

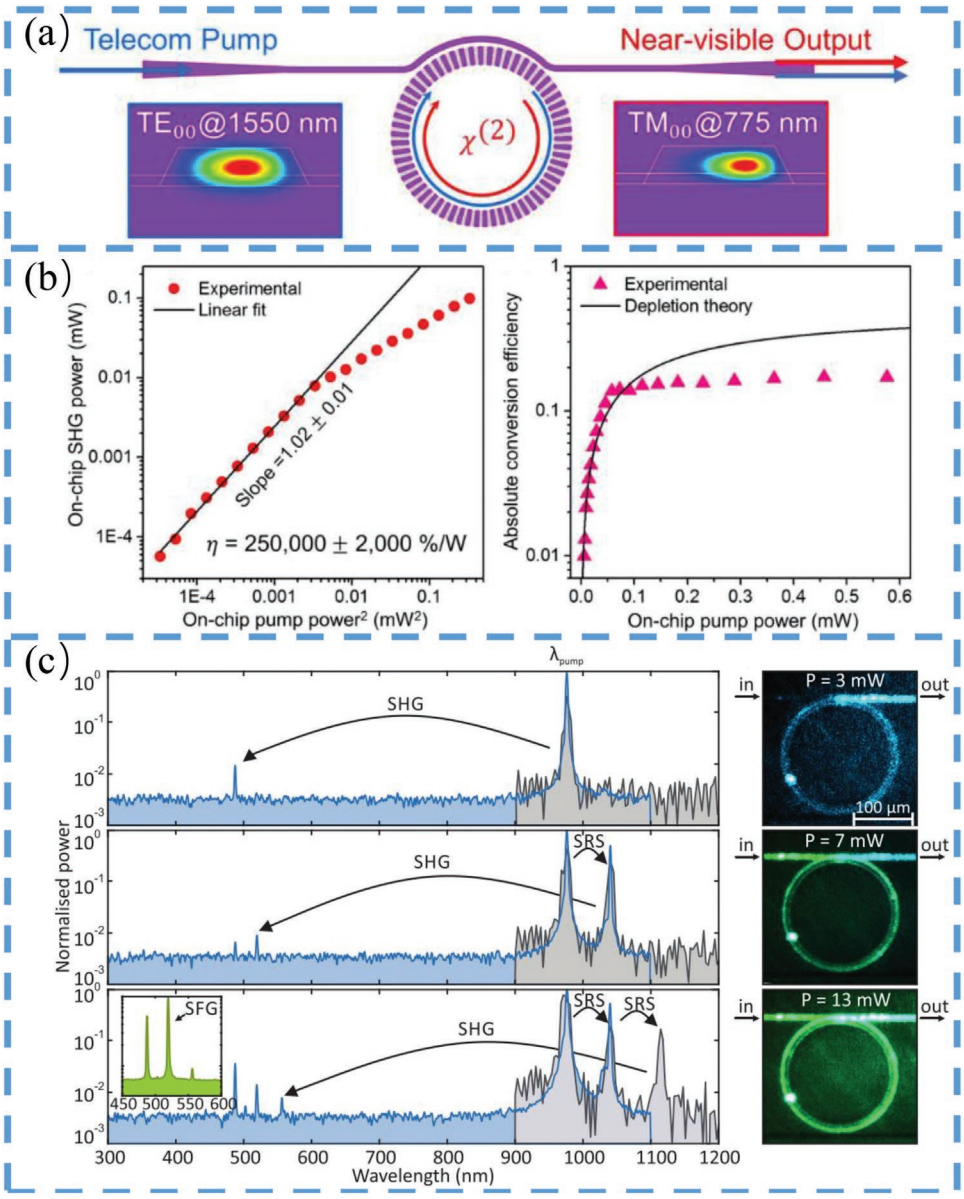

Figure 8. a) Schematic of the experiment set-up with SHG efficiency about 250 000%/W. b) The power dependence of SHG power and the absolute conversion efficiency. Reproduced with permission.[101] Copyright 2019, The Optical Society. c) Spectra of the cascaded scattered light and microscope images from top view with different pump light power. Reproduced with permission.[59] Copyright 2017, The Optical Society.

exhibited a higher EO modulation efficiency even in a z-cut LN wafer.

3.3. Frequency Combs

Frequency combs comprising a series of equidistant sidebands in spectra, have been regarded as an ultra precise ruler and harnessed in a wide range of applications like spectroscopy, shaping and detections. In the early days, conventional frequency combs have been realized from mode-locked femtosecond lasers.[130] Later, optical microresonators have emerged as a novel source to propel the miniaturization of frequency combs into on-chip devices so as to work compatible to the portable and monolithic development in photonic circuits.[31,131–134] For building frequency combs, besides high quality factors to enable the cascaded frequency conversion at low thresholds, the dispersion of optical microresonators also needs to be carefully engineered for extending the bandwidth of combs. This is because dispersion leads to the variation of free spectral range (FSR, the spectral distance between two neighbouring longitudinal resonant modes). The farther comb line frequencies escape from pump laser frequency, the less enhancement from cavities they can get because of off-resonance. Thus the dispersion of cavities is generally required as a flat curve to widen the comb bandwidth. To characterize the impact of dispersion inside cavities, the resonance frequencies ω_μ can be written as a Taylor expansion around the pump frequency ω_0

Table 2. Experimental parameters for microresonator EO modulators in published literatures.

Type	Material	Tuning rate [pm/V]	Cut-direction	Mode polarization	Ref.
Ring	LN	1.05	z	TM	[66]
Ring	LN/Si	12.5	z	TM	[118]
Ring	LN/Si	3.3	z	TE	[119]
Disk	LN	3.41	x	–	[120]
Racetrack	LN	0.32	y	TE	[121]
Ring	LN	7	x	TE	[122]
Racetrack	LN/Si_3N_4	2.9	x	TE	[123]
Ring	LN/Si_3N_4	1.78	x	TE	[124]
Disk	LN	0.38	x	–	[125]
Ring	LN	3	z	TM	[126]
Ring	LN	2.4	x	TE	[127]
Disk	LN	29.2	z	TE	[64]

as $\omega_\mu = \omega_0 + D_1\mu + \frac{1}{2}D_2\mu^2 + \frac{1}{6}D_3\mu^3 + \cdots$, where μ is the longitudinal resonance mode number, D_1 equals the FSR with the absence of dispersion, D_2 is relative to the group-velocity dispersion (GVD) β_2 with $D_2 = -\frac{c}{n}D_1^2\beta_2$.[135,136] The total nonlinear dispersion terms can be represented as $D_{int} = \omega_\mu - \omega_0 - D_1\mu$, quantifying the shifting from FSR resulted from dispersion, which is a key value to be considered when considering frequency combs as long as solitons.

There is a prevalent type of frequency combs called Kerr frequency combs[131,132] generated from cascaded four wave mixing process ($\chi^{(3)}$), where the signal and idler frequencies coincide with resonance modes with distance of FSRs. To counteract the influence from self-phase modulation as well as crossing

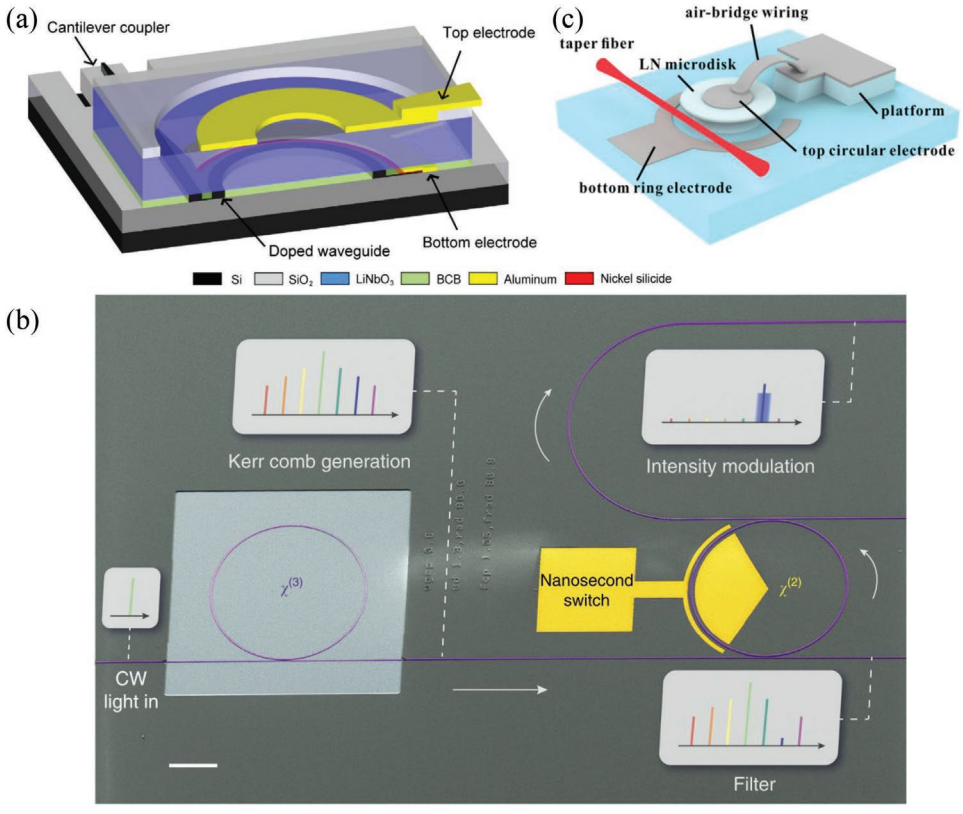

Figure 9. a) Schematic of the hybrid silicon and $LiNbO_3$ microring EO modulator. Reproduced with permission.[119] Copyright 2014, The Optical Society. b) An electro-optically tuneable add-drop filter in the monolithic integrated photonic circuit. Reproduced with permission.[127] Copyright 2019, Springer Nature. c) 3D view of $LiNbO_3$ microdisk EO modulator. Reproduced with permission.[64] Copyright 2020, Institute of Electrical and Electronics Engineers.

phase modulation, anomalous GVD ($\beta_2 < 0$ or $D_2 > 0$) is one requirement to accomplish parametric oscillation gain in Kerr frequency combs,[137] which asks for an elaborate geometry design of microresonators to compensate the usually normal GVD from materials. In detail, the curve of D_{int} versus mode number μ in one mode family should be a parabola with the opening toward up for anomalous GVD. No fluctuation around the pump frequency is expected as the mode crossing may cancel the formation of solitons.[135] In 2018, He et al. studied the dispersion in LN microring resonators and demonstrated the GVD from normal to anomalous regimes by adjusting the ring cross sections,[61] which pointed the feasibility of LN thin film microresonators on various nonlinear photonic applications including Kerr frequency combs. Recently, the migration of Kerr frequency combs in LN thin film microresonators has been demonstrated in several groups.[125,127,138–141] Benefiting the perfect behaviour in EO modulation, LN microresonators paved a practical step toward tunable frequency combs.[125,127] By utilizing the emission of dual dispersion waves, Gong et al. spanned the Kerr cavity soliton bandwidth up to 4/5 octaves in a microring resonator produced by the z-cut LN thin film.[140] **Figure 10**a shows observed spectra of the single-soliton and two-soliton microcombs, which features a sub-terahertz (THz) repetition rate of 335 GHz and a total span of 112 THz. The existence of these two dispersion waves (separated by 2/3 octaves) accumulated more light energy around the edges resulting in the extension of the whole comb spectrum. They also investigated how the profile of the integrated dispersion curve impacted on the Kerr frequency combs. Due to dispersion mainly depending on the geometry and refractive index, here the dimensions of microrings including radius, thickness and top width were engineered. Further, Yu et al. focused on the interaction of Kerr frequency combs and Raman scattering, helping provide clear insight to these nonlinear effects as well as practical suggestions in applications.[141]

Although Kerr frequency comb has been achieved from the near- to mid-infrared portions of the spectrum, the intricate underlying physics hinders its progress as the lacking in stability and controllability. Another alternative solution is the EO comb taking advantages of the strong quadratic nonlinearity ($\chi^{(2)}$), which possesses impressive zoom for modifications, such as flexible sidebands spacing and power. During the generation process, the electrodes need to be loaded under a microwave signal whose modulation frequency equals with the FSR of the

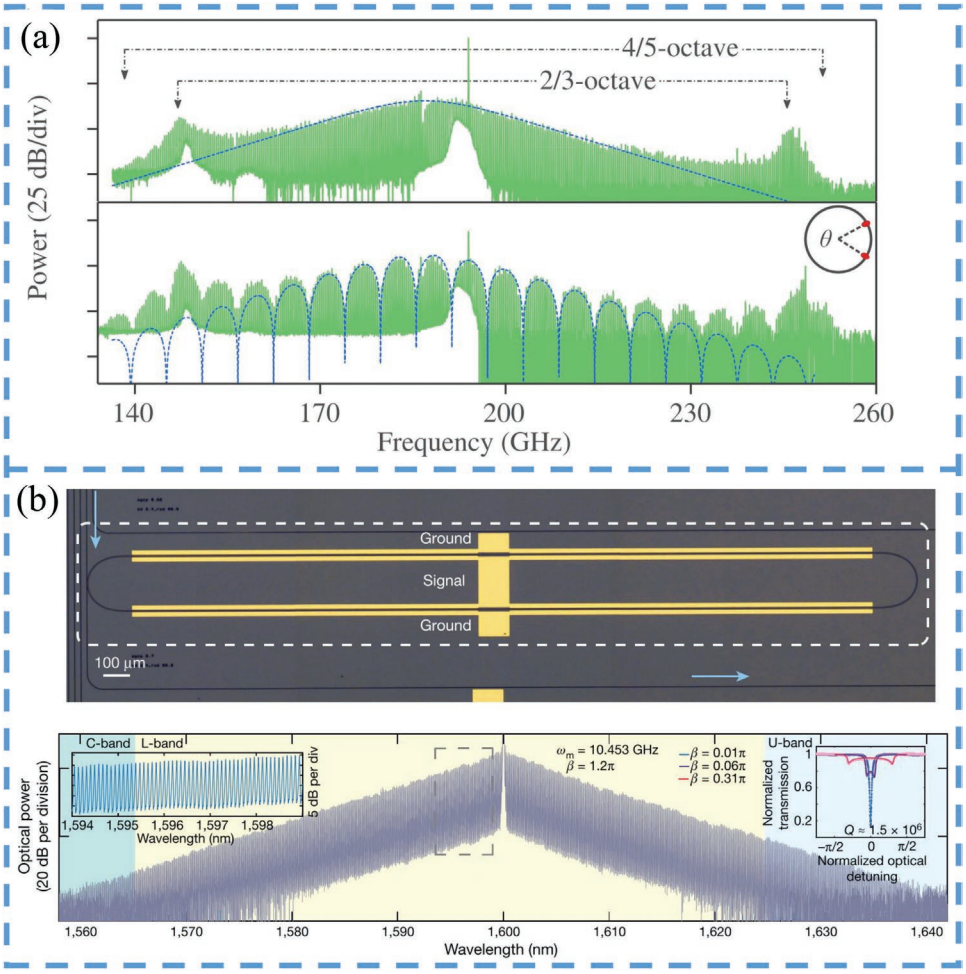

Figure 10. a) Kerr comb generator: spectra of single-soliton (upper) and dual-soliton (lower) states. Reproduced with permission.[140] Copyright 2020, The Optical Society. b) EO comb generator: micrograph of a fabricated lithium niobate microring resonator with gold microelectrodes (upper) and the output spectrum exceeding 80nm. Reproduced with permission.[142] Copyright 2019, Springer Nature.

microresonator. The sideband caused from the EO modulation can be confined again in the cavity as this sideband lies in another resonant modes location. After keeping repeating such process, the comb spectrum appears. The EO comb based on the LN thin film microresonators was recognized with a broad comb span over the whole telecommunications L-band, consisting of more than 900 separated frequencies with a 10.453 GHz space,[142] seen as Figure 10b. Conventional microresonator materials like silica or silicon only possess the third-order nonlinearity as frequency comb generation source, while the strong second-order nonlinearity endows LN the candidate for EO frequency combs based on lower-order nonlinearity followed with less complexity and higher stability, which may be another hotspot in the development of frequency comb generator.

3.4. Microwave-to-Optical Transducers

Microwave-to-optical transducers are important roadblocks for quantum networks owing to the pressing requirement for connecting the superconducting circuits at microwave working wavelength to the long distance communication in telecom optical wavelength. Benefited from its excellent optical and mechanical qualities as long as large electronic bandgaps, LN is doomed to a promising platform for microwave-to-optical conversion. A common demonstration is harnessing optomechanics where mechanical modes bridge microwave to optical lights via piezoelectric effect and photoelastic effect. Possessing low-loss optical WGMs and mechanical breathing modes, free-standing microdisks have been firstly explored for optomechanics.[69,72] Later on, the development of fabrication techniques makes it possible to suspend LN thin film microrings for free mechanical modes. On-chip microrings are more suitable to complex integrated devices, which is a further step toward large-scale quantum photonic networks. By employing the film thickness mode on the thin film LN platform, a mechanical resonance up to 5.2 GHz has been achieved in microrings, whose frequency-quality factor product of 6.6×10^{13} is the state-of-the-art value.[145] Shao et al. fabricated acousto-optic racetrack microresonator in LN thin film, based on which an optomechanical single-photon coupling strength of 1.1 kHz and a photon number conversion efficiency of 0.0017% was reported. Here microwave information was input by an interdigital transducer (IDT) and then emitted the acoustic modes to give impact on the output optical modes (**Figure 11**a).[143]

Although much progress has been realized in microwave-to-optical transducers based on mechanical modes, the introduction of another mediate also obstacles the applications to some degree. For example, the low resonance frequency of mechanical modes situates this kind of transducer very sensible to thermal noises and any low-frequency technical noises, which deeply limits its robustness in future applications. Besides, the demand of free-standing structures not only complicates the fabrication process but also further reduces the stability practically. As an alternative solution, direct transducer based on EO effect was proposed benefiting from an ingenious design,[146] which has also been achieved in experiment by the same group.[144] In this case, two LN thin film microrings were evanescently coupled turning a Lorentzian dip into a doublet transmission. The microwave input signal modified these two superposition modes and collaborated with the pumping light to up-convert into the output target optical modes. As shown in Figure 11b, the maximal conversion efficiency approached was 2.7×10^{-5}. Apart from the merit of robustness, the splitting of doublet can be simply controlled by a bias voltage applied, providing this kind of EO transducers with more tunable room for various microwave information.

3.5. Quantum Photonics

Photons are key ingredients in quantum information processing for its advantages in fast and long propagation and potential of infinite-dimensional Hilbert spaces. It is for this reason that quantum photonic circuits has been of great interest to fully capitalize photons for quantum revolution. Among various platforms, LN stands out because of its various reconfigured modulation and low thresholds of nonlinear optical effects. There are a series of significant breakthroughs achieved on LN thin film microresonators: quantum photon source,[71,147] quantum analogue,[148] single-photon nonlinear anharmonicity[149] and quantum controlled-Z quantum gate.[150]

Primarily driven by our focus, here we choose two experiments to introduce LN thin film microresonators' prospect in quantum source and quantum analogue. In a z-cut periodically poled LN thin film microring resonator, an unprecedented spontaneous parametric down-conversion efficiency was approached by utilizing three fundamental resonant modes and the highest nonlinear coefficient (d_{33}), ultimately offering the generation for quantum optical sources.[147] A quasi-TM fundamental mode in visible band was pumped to excite another two modes as signal and idler light in infrared band via spontaneous parametric down-conversion. This demonstration reached a high photon-pair generation rate of 2.7 MHz per microwatt of pump power, making orders of magnitude enhancement across all material platforms. Heralded generation of single photons was also measured corresponding with an 8.5 MHz rate and 0.008 autocorrelation (**Figure 12**a). These results have successfully proved the abundant superiority of LN to generate single photon as well as photon-pairs, which is the basis of quantum information processing. In addition, finding proper optical analogue contributes considerably in understanding complex underlying physics behind charming quantum effects. Coupled microresonators, also well known as photonic molecules, are excellent platforms to work in parallel to canonical two-level atomic system. Recently, the photonic molecule was transplanted into LN thin film microresonators with the use of elaborate EO modulation. During the experiment, not only a wide range of quantum effects including Autler-Townes splitting, Stark shift and Ramsey interference were realized, but also fine photon storage and retrieval were observed, which was definitely a milestone in quantum information processing (Figure 12b).[148]

3.6. Lasing

Owing to the stable optical transition and long lifetime, rare-earth ions (Er^{3+}, Yb^{3+}, Tm^{3+}, etc) are often doped in optical

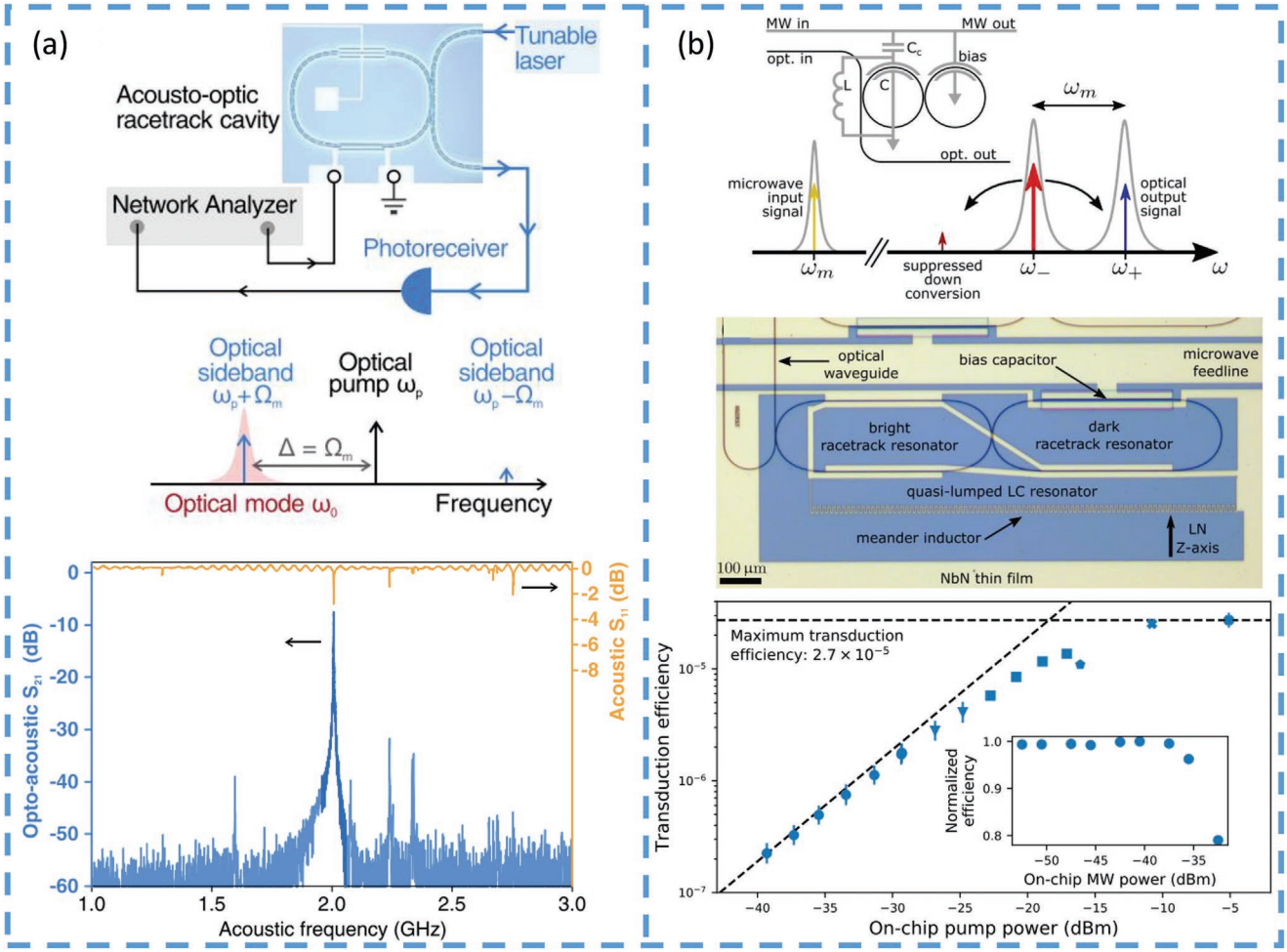

Figure 11. a) The acousto-optic racetrack transducer: simplified experimental schematic (top), principal illustration (center) and acoustic S_{11} and opto-acoustic S_{21} spectra (bottom). Reproduced with permission.[143] Copyright 2019, The Optical Society. b) Superconducting cavity electro-optic transducer: schematic and illustration (top), optical micrograph of the chip (center), maximal transduction efficiency when sweeping the bias voltage versus optical pump powers (bottom). Reproduced with permission.[144] Copyright 2020, The Optical Society.

microresonators to obtain active gain at an ultra-low pump threshold. Similar to other materials, LN also possesses the ability to host rare-earth ions, opening the avenue to active devices like microlasers and amplifiers.

To date, several groups in the world have already invested the qualities of rare earth-implanted LN microresonators.[151–157] For lacking of enough ion implantation concentration, the early experiments focused on the non-resonant fluorescence without laser output at cryogenic temperature, even the Q-factor being already above 10^5 (**Figure 13**a).[151,154] Among all the rare-earth ions, Er^{3+} is the most prevalent option as its optical transition lies in telecom band. Microlaser on erbium-doped LN thin film microresonators was achieved by three groups.[152,153,156] The erbium doped concentration they used was ranging from $0.1 mol\%$ to $1 mol\%$, approaching the lasering threshold below than 2.99 mW. The highest Q-factor was reported as 1.26×10^6, corresponding to the conversion efficiency of $6.5 \times 10^{-5}\%$, (Figure 13b).[152] Except the transduction from 970 nm (1460 nm) band to C band, up-conversion in energy levels also occurs which can be proved by the visible emission observed (Figure 13c).[153] However, the generation of visible emission consumes the energy from the pump light, which partly lifts the threshold for lasing. Another restriction in establishing low-loss microlaser comes from the photorefractive effect. To handle this, MgO can be embed meanwhile to mitigate photorefractive effect.

4. Summary and Outlook

This review focuses on the forefront of LN thin film based microresonators, ranging from the mainly used techniques during fabrication and characterization to a few of innovational applications. These novel applications selected here include frequency conversion, electro-optic modulation, frequency combs, microwave-to-optical transducers, quantum photonics and lasing. It should be noted that we reluctantly skip many ongoing novel developments, for example, the nontrivial studies in photorefractive effects[158–162] which help understand the principles of damages so as to improve the handing stability of photonic devices.

Despite tremendous novel demonstrations have appeared and shown abundant promises, the study of LN thin film

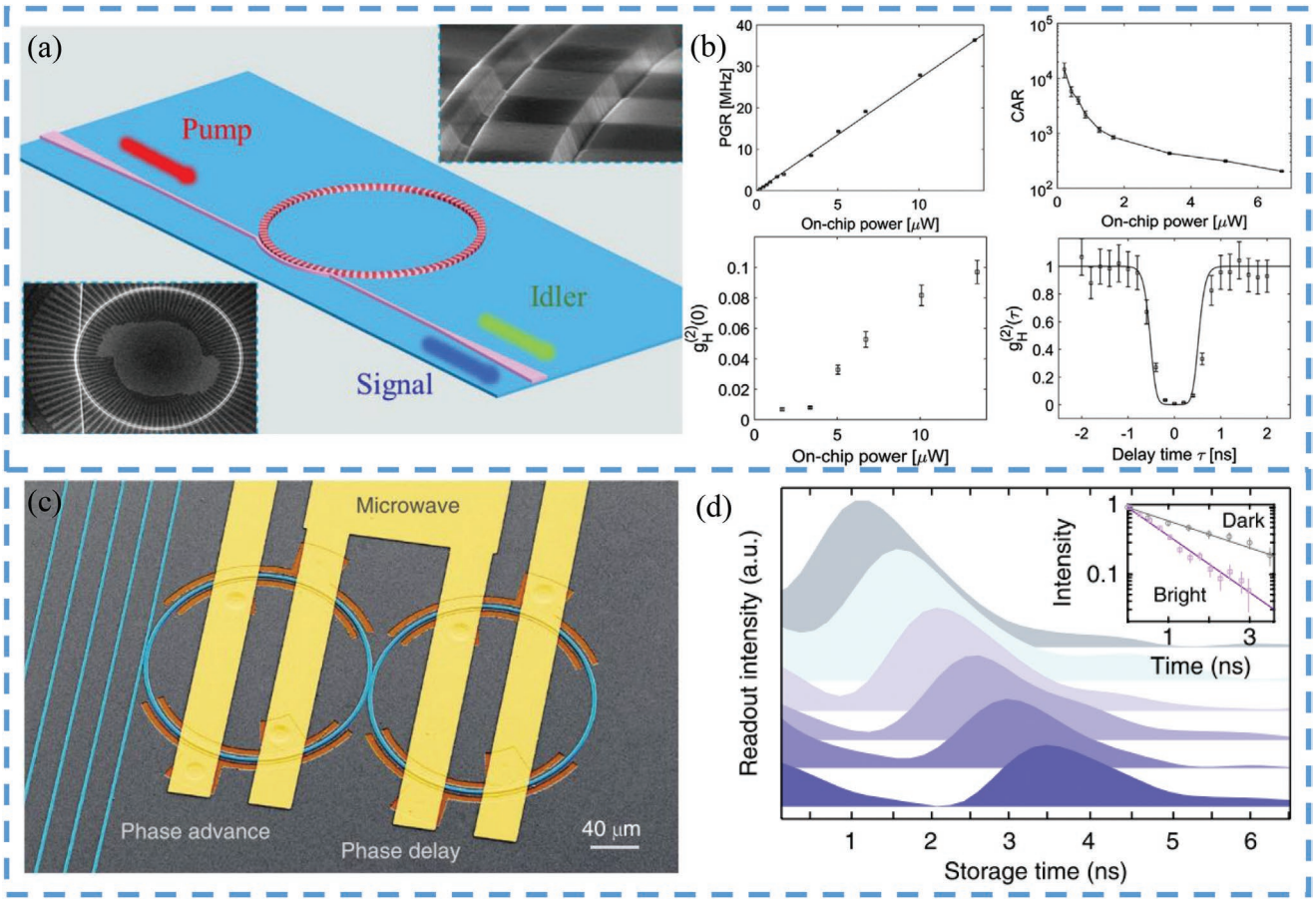

Figure 12. Quantum photon sources: a) schematic of the PPLN microring. Insets are SEM images of on-chip devices; b) photon-pair generation and heralded single-photon generation characterized by pair generation rate, coincidences-to-accidental ratio and autocorrelation function. Reproduced with permission.[147] Copyright 2020, The American Physical Society. Photonic molecule: c) false-coloured SEM image of coupled microrings; d) the intensity of the retrieved light at different time delays with the inset representing the compare between the dark and bright modes. Reproduced with permission.[148] Copyright 2019, Springer Nature.

based microresonators is still in its infancy, and many efforts are still highly demanded. To capitalize the merits of LN thin film microresonators, further optimization in fabrication, phase matching, and optical/electrical interface are requested to increase the utilization efficiencies, which is significant to steepen novel physical studies and create optical devices in the platforms of LN thin film based microresonators. There may be several future research directions of LN thin film based microresonators, which are summarized in follows.

Some traditional fields based on microresonators like non-reciprocity, sensing, and polarization are almost in vacant, where LN thin film based microresonators are capable to bloom. Associated with strong nonlinear performance and free EO modulation, LN thin film is bringing renewed potential to the realm of non-reciprocity. As yet, optical non-reciprocity has already been realized based on nonlinear frequency conversion in a PPLN thin-film waveguide.[163] Nevertheless, no such experimental demonstration have been reported in LN thin film based microresonators. Under the ultra-high incavity light energy, it can be envisioned to approach a considerably decreased threshold for exciting the unidirectional blocking. Sensing is one of the major applications of microresonators due to their narrow linewidth and subsequently high sensitivity. With the enhancement of Q factor of LN thin film based microresonators, this vast potential is doom to attract interest in sensing community.[164] Furthermore, heterogeneous structures compounded with diverse 2D layered materials[165] can expand their sensing application into broader and more sensitive areas such as biosensing and photodetection.

The development of active devices is still promising. Rare-earth ions doped LN thin film microresonators is in an initial stage with limited work wavelength. As mentioned in Section 3.6, nowadays only Er^{3+} ions have been successfully doped into LN thin film resonators to realize micro-lasers. With diverse ions being utilized and detailed studies being carried out, micro-lasers with broader output wavelength and lower threshold can be equipped for wider actual requirements in laser, amplifiers, and repeaters.[166–168] Beyond the lasing attempts, there is an absence of further researches by exploiting the gain in LN thin-film cavity systems. For example, microresonators are significant platforms to explore a variety of unconventional non-Hermitian effects by means of balancing gain and loss.[169] Since LN thin-film microresonators own rich modulation resources, this kind of non-Hermitian

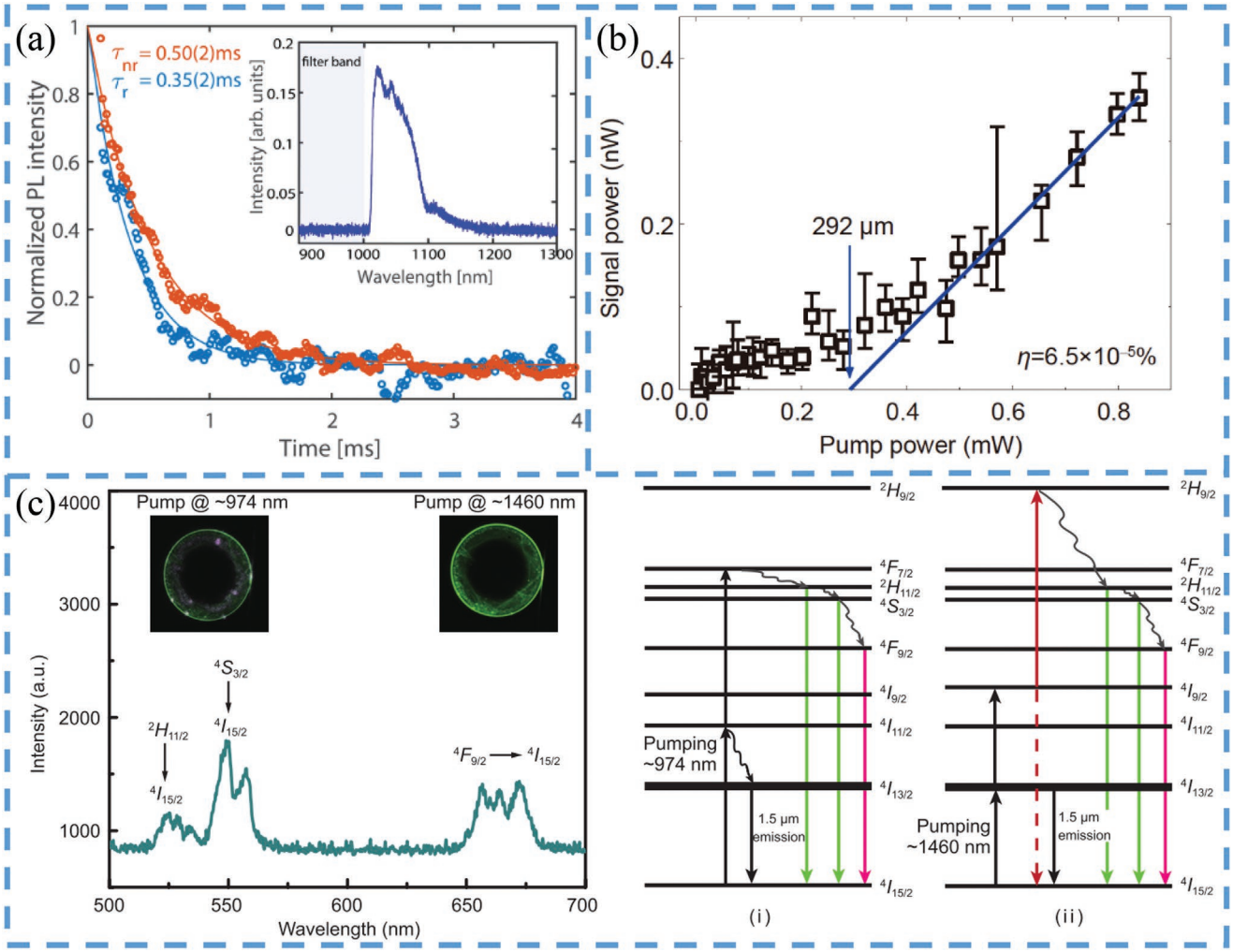

Figure 13. a) Two PL decay curves of Yb^{3+} ions measured at 4 K from the LN ring resonator. Reproduced with permission.[151] Copyright 2020, American Institute of Physics. b) The lasing signal intensity versus pumping power, giving the threshold of 292 μW and the conversion efficiency of 6.5×10^{-5}%. Reproduced with permission.[152] Copyright 2020, Springer Nature. c) Left panel: visible emission spectrum at 974-nm pumping of the Er^{3+}-doped LNOI microdisk, with the optical microscopy images of green emission; right panel: energy levels and optical transition with 974 nm and 1460 nm pumping. Reproduced with permission.[153] Copyright 2020, Springer Nature.

phenomenon are more accessible thanks to a decrease of operation difficulty. Besides, quantum dots can also be employed in LN thin film microresonators, which paves a way to controllable quantum emitters.

LN, famous as "silicon in photonics," is regarded as one of the most competitive candidate for integrated photonic circuits and complex quantum network.[170] In a monolithic system, miroresonators are crucial devices and further cooperation with other components as long as other materials should be investigated for the aim of multi-function, miniaturization, and energy conservation. In conjunction with additional electrical/RF elements, LN thin-film microresonators opens the avenue to versatile programmable modulators and transducers on chips. Combined with gain materials (rare-earth ions, quantum dots) or photodetective structures (2D layered materials, superconducting nanowires), both the source and the detection modules can be achievable. Besides, coupled LN thin film microresonators are useful artificial molecules to analogue colourful quantum effects and composite the necessary high-fidelity quantum gates.

In summary, as a perfect combination of light confinement and novel performances, LN thin film microresonators not only have already enriched the usefulness of microresonators in nonlinear optics and quantum photonics, but also would be doomed to propel the tremendous development of large-scale integrated photonic circuits and quantum networks.

Acknowledgements

This work was supported by National Natural Science Foundation of China (61727801), National Key Research and Development Program of China (2017YFA0303700, 2019YFA0705000), The Key Research and Development Program of Guangdong Province (2018B030325002), Beijing Innovation Center for Future Chip, and Tsinghua University Initiative Scientific Research Program. The authors thank Ruofei Xing for his help with the figures.

Conflict of Interest

The authors declare no conflict of interest.

Keywords

lithium niobate thin films, microresonators, nonlinear optics

Received: March 16, 2021
Revised: May 17, 2021
Published online:

[1] K. J. Vahala, *Nature* **2003**, *424*, 839.
[2] F. Lei, J. M. Ward, P. Romagnoli, S. Nic Chormaic, *Phys. Rev. Lett.* **2020**, *124*, 103902.
[3] L. Wu, H. Wang, Q. Yang, Q. xin Ji, B. Shen, C. Bao, M. Gao, K. Vahala, *Opt. Lett.* **2020**, *45*, 5129.
[4] L. He, Özdemir Şahin Kaya, L. Yang, *Laser Photonics Rev.* **2013**, *7*, 60.
[5] X.-F. Jiang, C.-L. Zou, L. Wang, Q. Gong, Y.-F. Xiao, *Laser Photonics Rev.* **2016**, *10*, 40.
[6] X. He, P. Liu, H. Zhang, Q. Liao, J. Yao, H. Fu, *Adv. Mater.* **2017**, *29*, 1604510.
[7] M. A. Bandres, S. Wittek, G. Harari, M. Parto, M. Khajavikhan, *Science* **2018**, *359*, 6381.
[8] W. E. Hayenga, M. Parto, J. Ren, F. O. Wu, M. P. Hokmabadi, C. Wolff, R. El-Ganainy, N. A. Mortensen, D. N. Christodoulides, M. Khajavikhan, *ACS Photonics* **2019**, *6*, 8.
[9] X. Yang, Şahin Kaya Özdemir, B. Peng, H. Yilmaz, F.-C. Lei, G.-L. Long, L. Yang, *Opt. Express* **2015**, *23*, 29573.
[10] T. Wang, M. Wang, Y.-Q. Hu, G.-L. Long, *EPL* **2018**, *124*, 14002.
[11] J.-h. Chen, X. Shen, S.-J. Tang, Q.-T. Cao, Q. Gong, Y.-F. Xiao, *Phys. Rev. Lett.* **2019**, *123*, 173902.
[12] J. Ma, L. Xiao, J. Gu, H. Li, X. Cheng, G. He, X. Jiang, M. Xiao, *Photonics Res.* **2019**, *7*, 573.
[13] C.-Z. Chai, H.-Q. Zhao, H. X. Tang, G.-C. Guo, C.-L. Zou, C.-H. Dong, *Laser Photonics Rev.* **2020**, *14*, 1900252.
[14] Q. T. Cao, R. Liu, H. Wang, Y. K. Lu, Y. F. Xiao, *Nat. Commun.* **2020**, *11*, 1136.
[15] M. Aspelmeyer, T. J. Kippenberg, F. Marquardt, *Rev. Mod. Phys.* **2014**, *86*, 1391.
[16] C. Dong, J. Zhang, V. Fiore, H. Wang, *Optica* **2014**, *1*, 425.
[17] J. Kim, M. C. Kuzyk, K. Han, H. Wang, G. Bahl, *Nat. Phys.* **2015**, *11*, 275.
[18] X. Jiang, M. Wang, M. C. Kuzyk, T. Oo, G.-L. Long, H. Wang, *Opt. Express* **2015**, *23*, 27260.
[19] S. Kim, J. M. Taylor, G. Bahl, *Optica* **2019**, *6*, 1016.
[20] Ş. K. Özdemir, J. Zhu, X. Yang, B. Peng, H. Yilmaz, L. He, F. Monifi, S. H. Huang, G. L. Long, L. Yang, *Proc. Natl. Acad. Sci.* **2014**, *111*, E3836.
[21] Y. Zhi, X. C. Yu, Q. Gong, L. Yang, Y. F. Xiao, *Adv. Mater.* **2017**, *29*, 1604920.
[22] Y. Wang, S. Zeng, G. Humbert, H.-P. Ho, *Laser Photonics Rev.* **2020**, *14*, 2000135.
[23] Y. H. Lai, Y. K. Lu, M. G. Suh, Z. Yuan, K. Vahala, *Nature* **2019**, 65.
[24] B. Peng, Özdemir Şahin Kaya, F. Lei, F. Monifi, L. Yang, *Nat. Phys.* **2014**, *10*, 394.
[25] T. Wang, Y.-Q. Hu, C.-G. Du, G.-L. Long, *Opt. Express* **2019**, *27*, 7344.
[26] C. Wang, X. Jiang, G. Zhao, M. Zhang, C. W. Hsu, B. Peng, A. D. Stone, L. Jiang, L. Yang, *Nat. Phys.* **2020**, *16*, 334.
[27] F. Zhang, Y. Feng, X. Chen, L. Ge, W. Wan, *Phys. Rev. Lett.* **2020**, *124*, 053901.
[28] R.-R. Xie, G.-Q. Qin, H. Zhang, M. Wang, G.-Q. Li, D. Ruan, G.-L. Long, *Opt. Lett.* **2021**, *46*, 773.
[29] X.-F. Liu, F. Lei, M. Gao, X. Yang, G.-Q. Qin, G.-L. Long, *Opt. Lett.* **2016**, *41*, 3603.
[30] X.-S. Xu, H. Zhang, M. Wang, D. Ruan, G.-L. Long, *Opt. Lett.* **2019**, *44*, 3250.
[31] M. Yu, Y. Okawachi, A. G. Griffith, N. Picque, M. Lipson, A. L. Gaeta, *Nat. Commun.* **2018**, *9*, 1869.
[32] L. Ren, X. Xu, S. Zhu, L. Shi, X. Zhang, *ACS Photonics* **2020**, *7*, 2995.
[33] J. Cardenas, M. Zhang, C. T. Phare, S. Y. Shah, C. B. Poitras, B. Guha, M. Lipson, *Opt. Express* **2013**, *21*, 16882.
[34] K. Powell, A. Shams-Ansari, S. Desai, M. Austin, J. Deng, N. Sinclair, M. Lončar, X. Yi, *Opt. Express* **2020**, *28*, 4938.
[35] Y. Zheng, M. Pu, A. Yi, X. Ou, H. Ou, *Opt. Lett.* **2019**, *44*, 5784.
[36] Y. Zheng, M. Pu, A. Yi, B. Chang, T. You, K. Huang, A. N. Kamel, M. R. Henriksen, A. A. Jørgensen, X. Ou, H. Ou, *Opt. Express* **2019**, *27*, 13053.
[37] C.-H. Chien, S.-H. Wu, T. H.-B. Ngo, Y.-C. Chang, *Phys. Rev. Applied* **2019**, *11*, 051001.
[38] R. S. Moirangthem, P.-J. Cheng, P. C.-H. Chien, B. T. H. Ngo, S.-W. Chang, C.-H. Tien, Y.-C. Chang, *Opt. Express* **2013**, *21*, 3010.
[39] C. Tessarek, R. Röder, T. Michalsky, S. Geburt, H. Franke, R. Schmidt-Grund, M. Heilmann, B. Hoffmann, C. Ronning, M. Grundmann, S. Christiansen, *ACS Photonics* **2014**, *1*, 990.
[40] Y. Zheng, C. Sun, B. Xiong, L. Wang, J. Wang, Y. Han, Z. Hao, H. Li, J. Yu, Y. Luo, in *Conf. on Lasers and Electro-Optics*, Optical Society of America, Washington, DC **2020**, p. SM4R.2.
[41] X. Han, W. Fu, C. Zhong, C. L. Zou, Y. Xu, A. A. Sayem, M. Xu, S. Wang, R. Cheng, L. Jiang, H. X. Tang, *Nat. Commun.* **2020**, *11*, 3237.
[42] A. W. Bruch, X. Liu, Z. Gong, J. B. Surya, M. Li, C.-L. Zou, H. X. Tang, *Nat. Photonics* **2020**, *15*, 21.
[43] R. S. Weis, T. K. Gaylord, *Appl. Phys. A* **1985**, *37*, 191.
[44] D. Janner, D. Tulli, M. Garcí-Granda, M. Belmonte, V. Pruneri, *Laser Photonics Rev.* **2009**, *3*, 301.
[45] F. Chen, *J. Appl. Phys.* **2009**, *106*, 081101.
[46] M. Bazzan, C. Sada, *Appl. Phys. Rev.* **2015**, *2*, 040603.
[47] V. Y. Shur, A. R. Akhmatkhanov, I. S. Baturin, *Appl. Phys. Rev.* **2015**, *2*, 040604.
[48] A. Boes, B. Corcoran, L. Chang, J. Bowers, A. Mitchell, *Laser Photonics Rev.* **2018**, *12*, 1700256.
[49] Y. Qi, Y. Li, *Nanophotonics* **2020**, *9*, 1287.
[50] J. Lin, F. Bo, Y. Cheng, J. Xu, *Photonics Res.* **2020**, *8*, 1910.
[51] D. Sun, Y. Zhang, D. Wang, W. Song, X. Liu, J. Pang, D. Geng, Y. Sang, H. Liu, *Light: Sci. Appl.* **2020**, *9*, 197.
[52] Y. Kong, F. Bo, W. Wang, D. Zheng, H. Liu, G. Zhang, R. Rupp, J. Xu, *Adv. Mater.* **2020**, *32*, 1806452.
[53] D. Zhu, L. Shao, M. Yu, R. Cheng, B. Desiatov, C. J. Xin, Y. Hu, J. Holzgrafe, S. Ghosh, A. Shams-Ansari, E. Puma, N. Sinclair, C. Reimer, M. Zhang, M. Lončar, *Adv. Opt. Photonics* **2021**, *13*, 242.
[54] M. Levy, R. M. Osgood, R. Liu, L. E. Cross, G. S. Cargill, A. Kumar, H. Bakhru, *Appl. Phys. Lett.* **1998**, *73*, 2293.
[55] G. Poberaj, H. Hu, W. Sohler, P. Günter, *Laser Photonics Rev.* **2012**, *6*, 488.
[56] Y. Jia, L. Wang, F. Chen, *Appl. Phys. Rev.* **2021**, *8*, 011307.
[57] NANOLN homepage, https://cn.nanoln.com/ (accessed: May 2018).
[58] J. Wang, F. Bo, S. Wan, W. Li, F. Gao, J. Li, G. Zhang, J. Xu, *Opt. Express* **2015**, *23*, 23072.
[59] R. Wolf, I. Breunig, H. Zappe, K. Buse, *Opt. Express* **2017**, *25*, 29927.

[60] M. Zhang, C. Wang, R. Cheng, A. Shams-Ansari, M. Lončar, *Optica* **2017**, *4*, 1536.
[61] Y. He, H. Liang, R. Luo, M. Li, Q. Lin, *Opt. Express* **2018**, *26*, 16315.
[62] J. Lin, N. Yao, Z. Hao, J. Zhang, W. Mao, M. Wang, W. Chu, R. Wu, Z. Fang, L. Qiao, W. Fang, F. Bo, Y. Cheng, *Phys. Rev. Lett.* **2019**, *122*, 173903.
[63] S. Liu, Y. Zheng, Z. Fang, X. Ye, Y. Cheng, X. Chen, *Opt. Lett.* **2019**, *44*, 1456.
[64] T.-J. Wang, G.-L. Peng, M.-Y. Chan, C.-H. Chen, *J. Lightwave Technol.* **2020**, *38*, 1851.
[65] R. Gao, H. Zhang, F. Bo, W. Fang, Z. Hao, N. Yao, J. Lin, J. Guan, L. Deng, M. Wang, L. Qiao, Y. Cheng, *arXiv:2102.00399*, **2021**.
[66] A. Guarino, G. Poberaj, D. Rezzonico, R. Degl'Innocenti, P. Günter, *Nat. Photonics* **2007**, *1*, 407.
[67] T.-J. Wang, J.-Y. He, C.-A. Lee, H. Niu, *Opt. Express* **2012**, *20*, 28119.
[68] C. Wang, M. J. Burek, Z. Lin, H. A. Atikian, V. Venkataraman, I.-C. Huang, P. Stark, M. Lončar, *Opt. Express* **2014**, *22*, 30924.
[69] W. C. Jiang, Q. Lin, *Sci. Rep.* **2016**, *6*, 36920.
[70] K. Zhang, Z. Chen, H. Feng, W.-H. Wong, E. Y.-B. Pun, C. Wang, *Chin. Opt. Lett.* **2021**, *19*, 060010.
[71] R. Luo, H. Jiang, H. Liang, Y. Chen, Q. Lin, *Opt. Lett.* **2017**, *42*, 1281.
[72] R. Wang, S. A. Bhave, in *Proc. of the Joint Conf. of the IEEE Int. Frequency Control Symp. and Int. Symp. on Applications of Ferroelectrics (IFCS-ISAF)*, IEEE, Piscataway, NJ **2020**, pp. 1–4.
[73] J. Lin, Y. Xu, Z. Fang, M. Wang, J. Song, N. Wang, L. Qiao, W. Fang, Y. Cheng, *Sci. Rep.* **2015**, *5*, 8072.
[74] J. Lin, Y. Xu, Z. Fang, M. Wang, N. Wang, L. Qiao, W. Fang, Y. Cheng, *Sci. China: Phys., Mech. Astron.* **2015**, *58*, 114209.
[75] M. Wang, R. Wu, J. Lin, J. Zhang, Z. Fang, Z. Chai, Y. Cheng, *Quantum Eng.* **2019**, *1*, e9.
[76] R. Wu, J. Zhang, N. Yao, W. Fang, L. Qiao, Z. Chai, J. Lin, Y. Cheng, *Opt. Lett.* **2018**, *43*, 4116.
[77] J. Zhang, Z. Fang, J. Lin, J. Zhou, M. Wang, R. Wu, R. Gao, Y. Cheng, *Nanomaterials* **2019**, *9*, 9.
[78] L. Ge, H. Jiang, Y. Liu, B. Zhu, C. Lu, Y. Chen, X. Chen, *Opt. Mater. Express* **2019**, *9*, 1632.
[79] P. Rabiei, J. Ma, S. Khan, J. Chiles, S. Fathpour, *Opt. Express* **2013**, *21*, 25573.
[80] A. N. R. Ahmed, S. Shi, A. J. Mercante, D. W. Prather, *Opt. Express* **2019**, *27*, 30741.
[81] F. Bo, J. Wang, J. Cui, Özdemir Şahin Kaya, Y. Kong, G. Zhang, J. Xu, L. Yang, *Adv. Mater.27*, 8075.
[82] M. Cai, O. Painter, K. J. Vahala, *Phys. Rev. Lett.* **2000**, *85*, 74.
[83] L. He, M. Zhang, A. Shams-Ansari, R. Zhu, C. Wang, L. Marko, *Opt. Lett.* **2019**, *44*, 2314.
[84] I. Krasnokutska, J.-L. J. Tambasco, A. Peruzzo, *Opt. Express* **2019**, *27*, 16578.
[85] N. Yao, J. Zhou, R. Gao, J. Lin, M. Wang, Y. Cheng, W. Fang, L. Tong, *Opt. Express* **2020**, *28*, 12416.
[86] Y. Pan, S. Sun, M. Xu, M. He, S. Yu, X. Cai, in *Conf. on Lasers and Electro-Optics*, Optical Society of America, Washington, DC **2020**, p. JTh2B.10.
[87] C. Hu, A. Pan, T. Li, X. Wang, Y. Liu, S. Tao, C. Zeng, J. Xia, *Opt. Express* **2021**, *29*, 5397.
[88] Z. Chen, Y. Wang, Y. Jiang, R. Kong, H. Hu, *Opt. Mater.* **2017**, *72*, 136.
[89] M. Bahadori, Y. Yang, L. L. Goddard, S. Gong, *Opt. Express* **2019**, *27*, 22025.
[90] L. Cai, G. Piazza, *J. Opt.* **2019**, *21*, 065801.
[91] A. Kar, M. Bahadori, S. Gong, L. L. Goddard, *Opt. Express* **2019**, *27*, 15856.
[92] S. Kang, R. Zhang, Z. Hao, D. Jia, F. Gao, F. Bo, G. Zhang, J. Xu, *Opt. Lett.* **2020**, *45*, 6651.
[93] I. Krasnokutska, R. J. Chapman, J.-L. J. Tambasco, A. Peruzzo, *Opt. Express* **2019**, *27*, 17681.
[94] B. Chen, Z. Ruan, J. Hu, J. Wang, C. Lu, A. P. T. Lau, C. Guo, K. Chen, P. Chen, L. Liu, *Opt. Express* **2021**, *29*, 1289.
[95] J. Y. Chen, Y. M. Sua, H. Fan, Y. P. Huang, *OSA Continuum* **2018**, *1*, 229.
[96] R. Luo, Y. He, H. Liang, M. Li, J. Ling, Q. Lin, *Phys. Rev. Appl.* **2019**, *11*, 034026.
[97] J. Lin, Y. Xu, J. Ni, M. Wang, Z. Fang, L. Qiao, W. Fang, Y. Cheng, *Phys. Rev. Appl.* **2016**, *6*, 014002.
[98] J. Lin, N. Yao, Z. Hao, J. Zhang, W. Mao, M. Wang, W. Chu, R. Wu, Z. Fang, L. Qiao, W. Fang, F. Bo, Y. Cheng, *Phys. Rev. Lett.* **2019**, *122*, 173903.
[99] R. Wolf, Y. Jia, S. Bonaus, C. S. Werner, S. J. Herr, I. Breunig, K. Buse, H. Zappe, *Optica* **2018**, *5*, 872.
[100] Z. Hao, L. Zhang, A. Gao, W. Mao, X. Lyu, X. Gao, F. Bo, F. Gao, G. Zhang, J. Xu, *Sci. China: Phys., Mech. Astron.* **2018**, *61*, 1.
[101] J. Lu, J. B. Surya, X. Liu, A. W. Bruch, Z. Gong, Y. Xu, H. X. Tang, *Optica* **2019**, *6*, 1455.
[102] Z. Hao, L. Zhang, W. Mao, A. Gao, X. Gao, F. Gao, F. Bo, G. Zhang, J. Xu, *Photon. Res.* **2020**, *8*, 311.
[103] J. Moore, J. K. Douglas, I. W. Frank, T. A. Friedmann, R. M. Camacho, M. Eichenfield, in *Conf. on Lasers and Electro-Optics*, Optical Society of America, Washington, DC **2016**, p. STh3P.1.
[104] G. Lin, J. U. Fürst, D. V. Strekalov, N. Yu, *Appl. Phys. Lett.* **2013**, *103*, 181107.
[105] J. A. Armstrong, N. Bloembergen, J. Ducuing, P. S. Pershan, *Phys. Rev.* **1962**, *127*, 1918.
[106] R. V. Gainutdinov, T. R. Volk, H. H. Zhang, *Appl. Phys. Lett.* **2015**, *107*, 162903.
[107] P. Mackwitz, M. Rüsing, G. Berth, A. Widhalm, K. Müller, A. Zrenner, *Appl. Phys. Lett.* **2016**, *108*, 152902.
[108] Z. Hao, J. Wang, S. Ma, W. Mao, F. Bo, F. Gao, G. Zhang, J. Xu, *Photonics Res.* **2017**, *5*, 623.
[109] X. Ye, S. Liu, Y. Chen, Y. Zheng, X. Chen, *Opt. Lett.* **2020**, *45*, 523.
[110] I. W. Frank, J. Moore, J. Douglas, R. Camacho, M. Eichenfield, in *Conf. on Lasers and Electro-Optics*, Optical Society of America, Washington, DC **2016**, p. SM2E.6.
[111] R. Luo, H. Jiang, S. Rogers, H. Liang, Y. He, Q. Lin, *Opt. Express* **2017**, *25*, 24531.
[112] J.-Y. Chen, Z.-H. Ma, Y. M. Sua, Z. Li, C. Tang, Y.-P. Huang, *Optica* **2019**, *6*, 1244.
[113] L. Zhang, D. Zheng, W. Li, F. Bo, F. Gao, Y. Kong, G. Zhang, J. Xu, *Opt. Express* **2019**, *27*, 33662.
[114] J. Lu, M. Li, C.-L. Zou, A. A. Sayem, H. X. Tang, *Optica* **2020**, *7*, 1654.
[115] S. Liu, Y. Zheng, X. Chen, *Opt. Lett.* **2017**, *42*, 3626.
[116] M. Wang, N. Yao, R. Wu, Z. Fang, S. Lv, J. Zhang, J. Lin, W. Fang, Y. Cheng, *New J. Phys.* **2020**, *22*, 073030.
[117] A. Rodriguez, M. Soljačić, J. D. Joannopoulos, S. G. Johnson, *Opt. Express* **2007**, *15*, 7303.
[118] L. Chen, M. G. Wood, R. M. Reano, *Opt. Express* **2013**, *21*, 27003.
[119] L. Chen, Q. Xu, M. G. Wood, R. M. Reano, *Optica* **2014**, *1*, 112.
[120] M. Wang, Y. Xu, Z. Fang, Y. Liao, P. Wang, W. Chu, L. Qiao, J. Lin, W. Fang, Y. Cheng, *Opt. Express* **2017**, *25*, 124.
[121] M. Mahmoud, L. Cai, C. Bottenfield, G. Piazza, *IEEE Photonics J.* **2018**, *10*, 1.
[122] C. Wang, M. Zhang, B. Stern, M. Lipson, M. Lončar, *Opt. Express* **2018**, *26*, 1547.
[123] A. N. R. Ahmed, S. Shi, A. J. Mercante, D. W. Prather, *Opt. Express* **2019**, *27*, 30741.
[124] A. N. R. Ahmed, S. Shi, M. Zablocki, P. Yao, D. W. Prather, *Opt. Lett.* **2019**, *44*, 618.

[125] Z. Fang, H. Luo, J. Lin, M. Wang, J. Zhang, R. Wu, J. Zhou, W. Chu, T. Lu, Y. Cheng, *Opt. Lett.* **2019**, *44*, 5953.
[126] I. Krasnokutska, J. L. J. Tambasco, A. Peruzzo, *Sci. Rep.* **2019**, *9*, 11086.
[127] C. Wang, M. Zhang, M. Yu, R. Zhu, H. Hu, M. Loncar, *Nat. Commun.* **2019**, *10*, 978.
[128] M. Bahadori, L. L. Goddard, S. Gong, *Opt. Express* **2020**, *28*, 13731.
[129] Z. Wang, C. Wu, Z. Fang, M. Wang, J. Lin, R. Wu, J. Zhang, J. Yu, M. Wu, W. Chu, T. Lu, G. Chen, Y. Cheng, *Chin. Opt. Lett.* **2021**, *19*, 060002.
[130] S. T. Cundiff, J. Ye, *Rev. Mod. Phys.* **2003**, *75*, 325.
[131] A. A. Savchenkov, A. B. Matsko, W. Liang, V. S. Ilchenko, D. Seidel, L. Maleki, *Nat. Photonics* **2011**, *5*, 293.
[132] T. J. Kippenberg, R. Holzwarth, S. A. Diddams, *Science* **2011**, *332*, 555.
[133] T. Herr, V. Brasch, J. D. Jost, C. Y. Wang, N. M. Kondratiev, M. L. Gorodetsky, T. J. Kippenberg, *Nat. Photonics* **2013**, *8*, 145.
[134] P. Marin-Palomo, J. N. Kemal, M. Karpov, A. Kordts, J. Pfeifle, M. H. P. Pfeiffer, P. Trocha, S. Wolf, V. Brasch, M. H. Anderson, R. Rosenberger, K. Vijayan, W. Freude, T. J. Kippenberg, C. Koos, *Nature* **2017**, *546*, 274.
[135] T. Herr, V. Brasch, J. D. Jost, I. Mirgorodskiy, G. Lihachev, M. L. Gorodetsky, T. J. Kippenberg, *Phys. Rev. Lett.* **2014**, *113*, 123901.
[136] S. Fujii, T. Tanabe, *Nanophotonics* **2020**, *9*, 1087.
[137] M. A. Foster, A. C. Turner, J. E. Sharping, B. S. Schmidt, M. Lipson, A. L. Gaeta, *Nature* **2006**, *441*, 960.
[138] Z. Gong, X. Liu, Y. Xu, M. Xu, J. B. Surya, J. Lu, A. Bruch, C. Zou, H. X. Tang, *Opt. Lett.* **2019**, *44*, 3182.
[139] Y. He, Q.-F. Yang, J. Ling, R. Luo, H. Liang, M. Li, B. Shen, H. Wang, K. Vahala, Q. Lin, *Optica* **2019**, *6*, 1138.
[140] Z. Gong, X. Liu, Y. Xu, H. X. Tang, *Optica* **2020**, *7*, 1275.
[141] M. Yu, Y. Okawachi, R. Cheng, C. Wang, M. Zhang, A. L. Gaeta, M. Loncar, *Light: Sci. Appl.* **2020**, *9*, 9.
[142] Mian , Zhang, Brandon , Buscaino, Cheng , Wang, Amirhassan , Shams-Ansari, Christian, R. and, *Nature* **2019**, *568*, 373.
[143] L. Shao, M. Yu, S. Maity, N. Sinclair, L. Zheng, C. Chia, A. Shams-Ansari, C. Wang, M. Zhang, K. Lai, M. Lončar, *Optica* **2019**, *6*, 1498.
[144] J. Holzgrafe, N. Sinclair, D. Zhu, A. Shams-Ansari, M. Colangelo, Y. Hu, M. Zhang, K. K. Berggren, M. Lončar, *Optica* **2020**, *7*, 1714.
[145] M. Shen, J. Xie, C.-L. Zou, Y. Xu, W. Fu, H. X. Tang, *Appl. Phys. Lett.* **2020**, *117*, 131104.
[146] M. Soltani, M. Zhang, C. Ryan, G. J. Ribeill, C. Wang, M. Loncar, *Phys. Rev. A* **2017**, *96*, 043808.
[147] Z. Ma, J.-Y. Chen, Z. Li, C. Tang, Y. M. Sua, H. Fan, Y.-P. Huang, *Phys. Rev. Lett.* **2020**, *125*, 263602.
[148] M. Zhang, C. Wang, Y. Hu, A. Shams-Ansari, T. Ren, S. Fan, M. Lončar, *Nat. Photonics* **2019**, *13*, 36.
[149] J. Lu, M. Li, C.-L. Zou, A. A. Sayem, H. X. Tang, *Optica* **2020**, *7*, 1654.
[150] M. Li, Y.-L. Zhang, H. X. Tang, C.-H. Dong, G.-C. Guo, C.-L. Zou, *Phys. Rev. Applied* **2020**, *13*, 044013.
[151] D. Pak, H. An, A. Nandi, X. Jiang, Y. Xuan, M. Hosseini, *J. Appl. Phys.* **2020**, *128*, 084302.
[152] Q. Luo, Z. Hao, C. Yang, R. Zhang, D. Zheng, S. Liu, H. Liu, F. Bo, Y. Kong, G. Zhang, J. Xu, *Sci. China: Phys., Mech. Astron.* **2020**, *64*, 234263.
[153] Y. Liu, X. Yan, J. Wu, B. Zhu, Y. Chen, X. Chen, *Sci. China: Phys., Mech. Astron.* **2020**, *64*, 234262.
[154] S. Wang, L. Yang, R. Cheng, Y. Xu, M. Shen, R. L. Cone, C. W. Thiel, H. X. Tang, *Appl. Phys. Lett.* **2020**, *116*, 151103.
[155] Z. Chen, Q. Xu, K. Zhang, W.-H. Wong, D.-L. Zhang, E. Y.-B. Pun, C. Wang, *Opt. Lett.* **2021**, *46*, 1161.
[156] Z. Wang, Z. Fang, Z. Liu, W. Chu, Y. Zhou, J. Zhang, R. Wu, M. Wang, T. Lu, Y. Cheng, *arXiv:2009.08953* **2020**.
[157] L. Yang, S. Wang, M. Shen, Y. Xu, J. Xie, H. X. Tang, *Opt. Express* **2021**, *29*, 15497.
[158] H. Jiang, R. Luo, H. Liang, X. Chen, Y. Chen, Q. Lin, *Opt. Lett.* **2017**, *42*, 3267.
[159] X. Sun, H. Liang, R. Luo, W. C. Jiang, X.-C. Zhang, Q. Lin, *Opt. Express* **2017**, *25*, 13504.
[160] Y. He, H. Liang, R. Luo, M. Li, Q. Lin, *Opt. Express* **2018**, *26*, 16315.
[161] J. B. Surya, J. Lu, Y. Xu, H. X. Tang, *Opt. Lett.* **2021**, *46*, 328.
[162] Y. Xu, A. A. Sayem, C.-L. Zou, L. Fan, R. Cheng, H. X. Tang, *Opt. Lett.* **2021**, *46*, 432.
[163] K. Abdelsalam, T. Li, J. B. Khurgin, S. Fathpour, *Optica* **2020**, *7*, 209.
[164] J. Zhang, Y. M. Sua, J.-Y. Chen, J. Ramanathan, C. Tang, Z. Li, Y. Hu, Y.-P. Huang, *Appl. Phys. Lett.* **2021**, *118*, 171103.
[165] Z. Sun, A. Martinez, F. Wang, *Nat. Photonics* **2016**, *10*, 227.
[166] X. Jiang, D. Pak, A. Nandi, Y. Xuan, M. Hosseini, *Appl. Phys. Lett.* **2019**, *115*, 071104.
[167] S. Dutta, E. A. Goldschmidt, S. Barik, U. Saha, E. Waks, *Nano Lett.* **2020**, *20*, 741.
[168] B. Wei, W.-H. Cai, C. Ding, G.-W. Deng, R. Shimizu, Q. Zhou, R.-B. Jin, *Opt. Express* **2021**, *29*, 256.
[169] Ş. K. Özdemir, S. Rotter, F. Nori, L. Yang, *Nat. Mater.* **2019**, *18*, 783.
[170] W. Bogaerts, D. Pérez, J. Capmany, D. Miller, J. Poon, D. Englund, F. Morichetti, A. Melloni, *Nature* **2020**, *586*, 207.

Ran-Ran Xie received her B.S. degree from Shandong University, Jinan, China, in 2016. She is now working toward a Ph.D. degree in the Department of Physics, Tsinghua University. Her research interests lie in whispering-gallery-mode microcavities, microcavity sensing and nonlinear optics.

Gui-Qin Li is now an associate professor of the Department of Physics, Tsinghua University. Her main research projects are theoretical calculation and experimental investigation of atomic, molecular, and optical physics, involved in structures, spectrum, and quantum control.

Feng Chen is currently a professor of the School of Physics, Shandong University. From 2003 to 2005, he was in the Clausthal University of Technology, Clausthal-Zellerfeld, Germany, as an Alexander von Humboldt Research Fellow. His research interests include femtosecond laser direct writing, optical waveguides, fabrication of micro-nanoscale photonic structures, nonlinear optics, and so forth. He is a Fellow of the Institute of Physics, U.K., a Fellow of SPIE, a senior member of the Optical Society of America, and a Director Board Member of the Chinese Physical Society.

Gui-Lu Long is a professor at Tsinghua University and Vice-President of Beijing Academy of Quantum Information Sciences. Notably among his contributions, he proposed the quantum secure direct communication (QSDC), constructed the Grover-Long algorithm for exact quantum search, the full quantum eigensolver (FQE) for NISQ applications; and established the widely used linear combination unitaries (LCU) method for quantum algorithm design. He proposed the WISE (Wavefunction Is System Entity) realistic interpretation of quantum mechanics. He is a fellow of IoP and APS. He was President of AAPPS, and vice-chair of C13 of IUPAP.